Channel Estimation for RIS-Aided Multi-User mmWave Systems With Uniform Planar Arrays

Zhendong Peng[®], Gui Zhou[®], Member, IEEE, Cunhua Pan[®], Member, IEEE, Hong Ren[®], Member, IEEE, A. Lee Swindlehurst[®], Fellow, IEEE, Petar Popovski[®], Fellow, IEEE, and Gang Wu[®], Member, IEEE

Abstract-In this paper, we adopt a three-stage based uplink channel estimation protocol with reduced pilot overhead for an reconfigurable intelligent surface (RIS)-aided multi-user (MU) millimeter wave (mmWave) communication system, in which both the base station (BS) and the RIS are equipped with a uniform planar array (UPA). Specifically, in Stage I, the channel state information (CSI) of a typical user is estimated. To address the power leakage issue for the common angles-of-arrival (AoAs) estimation in this stage, we develop a low-complexity onedimensional search method. In Stage II, a re-parameterized common BS-RIS channel is constructed with the estimated information from Stage I to estimate other users' CSI. In Stage III, only the rapidly varying channel gains need to re-estimated. Furthermore, the proposed method can be extended to multiantenna UPA-type users, by decomposing the estimation of a multi-antenna channel with J scatterers into estimating J singlescatterer channels for a virtual single-antenna user. An orthogonal matching pursuit (OMP)-based method is proposed to estimate the angles-of-departure (AoDs) at the users. Simulation results demonstrate that the proposed algorithm significantly achieves high channel estimation accuracy, which approaches the genie-aided upper bound in the high signal-to-noise ratio (SNR) regime.

Manuscript received 22 March 2022; revised 12 August 2022 and 23 September 2022; accepted 5 October 2022. Date of publication 14 October 2022; date of current version 19 December 2022. This work was supported in part by the National Natural Science Foundation of China (62101128) and Basic Research Project of Jiangsu Provincial Department of Science and Technology (BK20210205). This work has been supported in part by the U.S. National Science Foundation under grants ECCS-2030029 and CNS-2107182 and in part by the H2020 RISE-6G project. An earlier version of this paper will be presented at the IEEE Global Communications Conference, Rio de Janeiro, Brazil, December 2022 [1]. The associate editor coordinating the review of this article and approving it for publication was S. Ma. (Corresponding author: Cunhua Pan.)

Zhendong Peng and Gang Wu are with the National Key Laboratory of Science and Technology on Communications, University of Electronic Science and Technology of China, Chengdu 611731, China (e-mail: zhendong@std.uestc.edu.cn; wugang99@uestc.edu.cn).

Gui Zhou is with the Institute for Digital Communications, Friedrich-Alexander-University Erlangen–Nürnberg (FAU), 91054 Erlangen, Germany (e-mail: gui.zhou@fau.de).

Cunhua Pan and Hong Ren are with the National Mobile Communications Research Laboratory, Southeast University, Nanjing 210096, China (e-mail: cpan@seu.edu.cn; hren@seu.edu.cn).

A. Lee Swindlehurst is with the Center for Pervasive Communications and Computing, University of California at Irvine, Irvine, CA 92697 USA (e-mail: swindle@uci.edu).

Petar Popovski is with the Department of Electronic Systems, Aalborg University, 9220 Aalborg, Denmark (e-mail: petarp@es.aau.dk).

Color versions of one or more figures in this article are available at https://doi.org/10.1109/TCOMM.2022.3214892.

Digital Object Identifier 10.1109/TCOMM.2022.3214892

Index Terms—Reconfigurable intelligent surface, uniform planar array, millimeter wave, channel estimation.

I. Introduction

HANKS to its cost-effective, power-efficient and deployment-convenient features, reconfigurable intelligent surface (RIS) technology is envisioned to be a promising technique for enhancing the spectrum and energy efficiency of 6G-and-beyond communications systems [2], [3], [4], [5], [6], [7]. Deploying an RIS provides additional degrees-offreedom (DoF) that can be used to reconfigure the wireless propagation environment, which brings tremendous benefits for the wireless systems. To reap the benefits promised by RIS, accurate channel state information (CSI) is required [8], [9], [10], which is challenging to achieve for the following two reasons. First, an RIS equipped with passive elements typically does not have a receiver, so does not process complex baseband signals, which means that traditional channel estimation approaches cannot be adopted in RIS-aided systems. Due to this characteristic, it is not possible to estimate the user-RIS channel and RIS-base station (BS) channel separately, and instead the cascaded channel is estimated, i.e., the equivalent user-RIS-BS channel. Second, with a large number of antennas at the BS and reflecting elements at the RIS, the cascaded channel contains a large number of channel coefficients, which can require a larger number of pilots. Hence, developing an efficient channel estimation method for RIS-aided systems with low pilot overhead is imperative.

Recently, there have been many contributions on channel estimation for RIS-aided communication systems; see for example [11], [12], [13], [14], [15], [16], [17], [18] and the recent overview tutorial [8]. Early work focused mainly on unstructured channel models, but channel estimation for these models requires a pilot overhead that is proportional to the number of RIS reflecting elements, which is often prohibitively large. On the other hand, the sparse structure of high-frequency millimeter wave (mmWave) channels, described by the angles and gains of fewer paths, has been exploited to reduce the pilot overhead and improve the estimation accuarcy of multiple-input multiple-output (MIMO) systems efficiently by leveraging compressed sensing (CS) techniques, direction-of-arrival (DOA) estimation methods and Bayesian learning

0090-6778 © 2022 IEEE. Personal use is permitted, but republication/redistribution requires IEEE permission. See https://www.ieee.org/publications/rights/index.html for more information.

frameworks [19], [20], [21], [22]. Motivated by the works on structured channel models, the sparsity of the user-RIS-BS cascaded channel was exploited in [13] using CS to reconstruct the channel. The authors in [15] exploited the fact that the cascaded channel matrices for multiple users exhibit a common column-block sparsity since all users share the same RIS-BS channel, and developed an iterative channel estimator based on this observation. Inspired by the common columnblock sparsity property, the double-structured sparsity of the cascaded channel was considered in [16], using the Discrete Fourier Transform (DFT) to analyze the estimation of the angle parameters. The authors of [17] achieved a dramatic reduction in pilot overhead by fully utilizing the correlation among the different cascaded channels. The above-mentioned works [15], [16], [17] considered multiple users but assumed that they are equipped with only a single antenna. On the other hand, the RIS-aided MIMO scenario was considered in [13], [18], and [14]. The authors in [18] proposed an alternating minimization and manifold optimization (MO) estimation protocol for this scenario. To increase the estimation accuracy, a superresolution CS technique based on atomic norm minimization was applied to cascaded channel estimation in [14]. However, these three works assumed only a single user and thus did not take advantage of the inherent correlation among the channels of different users in an RIS-aided system. Apart from this, [13], [14], [16], [18] assumed that the number of scatterers for the user-RIS channel and RIS-BS channels are known a priori, i.e., the sparsity level is known. In practice, however, these parameters may not be known beforehand. Moreover, a uniform linear array (ULA)-type BS, ULA-type users and/or ULA-type RIS were assumed in the above mentioned works, which may not be relevant for RIS-assisted communication systems. The extension to the more typical uniform planar array (UPA)-type RIS-aided multi-user (MU) system is not straightforward. First, the number of angle parameters that must be estimated doubles that of a ULA-type system, and the asymptotic properties exploited for large ULAs may not be applicable. Second but important, increasing the number of parameters makes exploiting the channel correlation among multiple users extremely complex, especially for the cascaded channel parameters.

Against the above background, in this paper we propose an effective three-stage channel estimation method with low pilot overhead starting from an RIS-aided single-antenna MU mmWave communication system, in which the BS and RIS are both equipped with a UPA. Then, we extend the protocol to the multi-antenna user case, where the users are also equipped with UPAs. This is the first work that investigates the UPA-type MU MIMO case. The main contributions of this work are summarized as follows:

• We develop a three-stage uplink channel estimation protocol for an RIS-aided mmWave communication system with a multi-antenna UPA-type BS, a multi-element UPA-type RIS and multiple users. The protocol is divided into two parts: full CSI estimation in the first coherence block consisting of Stage I and Stage II, and estimation of updated gains in the remaining coherence blocks consisting of Stage III. In Stage I, only a typical user

sends pilots to the BS for channel estimation, from which we obtain estimated gains and angle information that is used to reduce the pilot overhead in the next stage. In particular, angle rotation operation is adopted to deal with the power leakage issue when estimating common AoAs in this stage. In Stage II, we exploit the correlation among different users' cascaded channels and construct a re-parameterized common RIS-BS channel using the estimated CSI of the typical user, based on which we obtain the channel estimates of other users. Next, in Stage III during the remaining coherence blocks, only the cascaded channel gains for different users are reestimated since the angle information remains constant.

- We propose an effective low-complexity one-dimensional (1-D) search method to achieve the angle rotation operation in Stage I. In [21], a two-dimensional (2-D) DFT together with a 2-D search method was used to compensate for the leaked power, which has high computational complexity. To reduce the complexity, we exploit the structure of the steering vectors at the BS and then introduce an equivalent Fourier matrix and rotation matrices to divide the 2-D search into two 1-D searches.
- We extend the estimation protocol to the case of users with UPAs. The angles-of-departure (AoDs) at the users and the common angles-of-arrival (AoAs) at the BS are estimated via the proposed orthogonal matching pursuit (OMP)-based method and DFT-based method, respectively. Then the estimation of a multi-antenna channel with J scatterers is decomposed into the estimation of J single-scatterer channels. The cascaded AoDs at the RIS and the channel gains can be estimated using methods similar to those developed for the single-antenna case. This is the first approach proposed in the literature that exploits the correlation between different users in the multi-antenna user case. The overall number of pilots for both the single- and multi-antenna case is also analyzed.

The rest of this paper is organized as follows. Section II introduces the system model and the three-stage based channel estimation protocol. Section III presents the full CSI estimation algorithm in Stage I and Stage II for the single-antennausers case. Channel gain estimation in Stage III is discussed in Section IV. Section V applies the protocol to the multi-antenna-users case. Simulation results are given in Section VI. Finally, Section VII concludes this work.

Notations: Vectors and matrices are denoted by boldface lowercase letters and boldface uppercase letters, respectively. For a matrix \mathbf{A} of arbitrary size, \mathbf{A}^* , \mathbf{A}^T , \mathbf{A}^H and \mathbf{A}^\dagger stand for the conjugate, transpose, conjugate transpose and pseudo-inverse of \mathbf{A} . For a square full-rank matrix \mathbf{A} , \mathbf{A}^{-1} denotes its inverse. The symbols $||\mathbf{A}||_F$, $||\mathbf{a}||$ represent the Frobenius norm of matrix \mathbf{A} and the Euclidean norm of vector \mathbf{a} , respectively. $\angle(\cdot)$ denotes the angle of a complex number. Diag $\{\mathbf{a}\}$ is a diagonal matrix with the entries of vector \mathbf{a} on its diagonal. $\mathrm{vec}(\mathbf{A})$ denotes the vectorization of \mathbf{A} obtained by stacking the columns of matrix \mathbf{A} . $\mathbb{E}\left\{\cdot\right\}$ denotes the expectation operation. $[\mathbf{a}]_m$ denotes the m-th element of the vector \mathbf{a} , and $[\mathbf{A}]_{m,n}$ denotes the (m,n)-th element of the matrix \mathbf{A} . The n-th column and the m-th row of matrix

A are denoted by $\mathbf{A}_{(:,n)}$ and $\mathbf{A}_{(m,:)}$ respectively. $\lceil a \rceil$ rounds up to the nearest integer. The inner product between two vectors \mathbf{a} and \mathbf{b} is denoted by $\langle \mathbf{a}, \mathbf{b} \rangle \triangleq \mathbf{a}^H \mathbf{b}$. Additionally, the Kronecker product, Hadamard product, Khatri-Rao product and transposed Khatri-Rao product between two matrices \mathbf{A} and \mathbf{B} are denoted by $\mathbf{A} \otimes \mathbf{B}$, $\mathbf{A} \odot \mathbf{B}$, $\mathbf{A} \diamond \mathbf{B}$ and $\mathbf{A} \bullet \mathbf{B}$, respectively. $\mathbf{i} \triangleq \sqrt{-1}$ is the imaginary unit.

II. SYSTEM MODEL AND ESTIMATION PROTOCOL

A. System Model

We consider a narrow-band time-division duplex (TDD) mmWave system, in which K single-antenna users communicate with a BS equipped with an $N=N_1\times N_2$ antenna UPA, where N_1 is the number of antennas in the vertical dimension, and N_2 in the horizontal dimension. To improve communication performance, an RIS equipped with a passive reflecting UPA of dimension $M=M_1\times M_2$ (M_1 vertical elements and M_2 hoirzontal elements) is deployed. The channels are assumed to be block-fading, and hence constant in each coherence block. In addition, we assume that the direct channels between the BS and users are blocked. Otherwise first estimate the direct channels by turning off the RIS, and then the cascaded channel can be estimated by removing the direct channel's contribution from the received signal.

The Saleh-Valenzuela (SV) model in [23] is used to represent the channels due to the limited scattering characteristics in the mmWave environment. Consider a typical $P=P_1\times P_2$ UPA whose steering vector $\mathbf{a}_P(z,x)\in\mathbb{C}^{P\times 1}$ can be represented by

$$\mathbf{a}_P(z,x) = \mathbf{a}_{P_1}(z) \otimes \mathbf{a}_{P_2}(x), \tag{1}$$

where $\mathbf{a}_{P_1}(z) = [1, e^{-\mathrm{i}2\pi z}, \dots, e^{-\mathrm{i}2\pi(P_1-1)z}]^\mathrm{T}$ and $\mathbf{a}_{P_2}(x) = [1, e^{-\mathrm{i}2\pi x}, \dots, e^{-\mathrm{i}2\pi(P_2-1)x}]^\mathrm{T}$ are the steering vectors with respect to z-axis (vertical direction) and x-axis (horizontal direction) of the UPA, respectively. The variables z and x can be regarded as the corresponding equivalent spatial frequency with respect to z-axis and x-axis of the UPA, respectively. Denote $\varrho \in [-90^\circ, 90^\circ)$ and $\xi \in [-180^\circ, 180^\circ)$ as the signal elevation and azimuth angles of the UPA, respectively. There exists a relationship between the spatial frequency pair (z,x) and the physical angle pair (ϱ,ξ) :

$$z = \frac{d}{\lambda_{-}}\cos(\varrho), \quad x = \frac{d}{\lambda_{-}}\sin(\varrho)\cos(\xi), \tag{2}$$

where λ_c is the carrier wavelength and d is the element spacing. Assuming that $d \leq \lambda_c/2$, there is a one-to-one relationship between the spatial frequencies and the physical angles on one side of the UPA. We will assume this relationship to hold in the remainder of the paper, and we will refer to the arguments of the steering vectors interchangeably as either angles or spatial frequencies.

Using the geometric channel model, the channel matrix between the RIS and the BS, denoted by $\mathbf{H} \in \mathbb{C}^{N \times M}$, and

¹The transposed Khatri-Rao product is known as the "row-wise Kronecker product", which utilizes the row-wise splitting of matrices with a given quantity of rows. Specifically, for given matrices $\mathbf{A} \in \mathbb{C}^{Q \times M}$ and $\mathbf{B} \in \mathbb{C}^{Q \times N}$, $\mathbf{A} \bullet \mathbf{B}$ is a $Q \times MN$ matrix of which each row is the Kronecker product of the corresponding rows of \mathbf{A} and \mathbf{B} .

the channel matrix between user k and the RIS, denoted by $\mathbf{h}_k \in \mathbb{C}^{M \times 1}$, can be written as

$$\mathbf{H} = \sum_{l=1}^{L} \alpha_l \mathbf{a}_N(\psi_l, \nu_l) \mathbf{a}_M^{\mathrm{H}}(\omega_l, \mu_l), \tag{3a}$$

$$\mathbf{h}_{k} = \sum_{j=1}^{J_{k}} \beta_{k,j} \mathbf{a}_{M}(\varphi_{k,j}, \theta_{k,j}), \quad \forall k \in \mathcal{K},$$
 (3b)

where L denotes the number of propagation paths (scatterers) between the BS and the RIS, and J_k denotes the number of propagation paths between the RIS and user k. In addition, α_l , (ψ_l, ν_l) and (ω_l, μ_l) are the complex path gain, AoA, and AoD of the l-th path in the RIS-BS channel, respectively. Similarly, $\beta_{k,j}$ and $(\varphi_{k,j}, \theta_{k,j})$ represent the complex path gain and AoA of the j-th path in the user k-RIS channel, respectively. Moreover, the channel models in (3) can be written in a more compact way as

$$\mathbf{H} = \mathbf{A}_N \mathbf{\Lambda} \mathbf{A}_M^{\mathrm{H}},\tag{4}$$

$$\mathbf{h}_k = \mathbf{A}_{M,k} \boldsymbol{\beta}_k, \quad \forall k \in \mathcal{K}, \tag{5}$$

where $\mathbf{A}_N = [\mathbf{a}_N(\psi_1, \nu_1), \dots, \mathbf{a}_N(\psi_L, \nu_L)] \in \mathbb{C}^{N \times L}$, $\mathbf{A}_M = [\mathbf{a}_M(\omega_1, \mu_1), \dots, \mathbf{a}_M(\omega_L, \mu_L)] \in \mathbb{C}^{M \times L}$ and $\mathbf{\Lambda} = \mathrm{Diag}\{\alpha_1, \dots, \alpha_L\} \in \mathbb{C}^{L \times L}$ are the AoA steering (array response) matrix, AoD steering matrix and complex gain matrix of the common RIS-BS channel, respectively, and $\mathbf{A}_{M,k} = [\mathbf{a}_M(\varphi_{k,1}, \theta_{k,1}), \dots, \mathbf{a}_M(\varphi_{k,J_k}, \theta_{k,J_k})] \in \mathbb{C}^{M \times J_k}$ and $\boldsymbol{\beta}_k = [\beta_{k,1}, \dots, \beta_{k,J_k}]^\mathrm{T} \in \mathbb{C}^{J_k \times 1}$ are the AoA steering matrix and complex gain vector of the specific user-RIS channel for user k, respectively.

Denote $\mathbf{e}_t \in \mathbb{C}^{M \times 1}$ as the phase shift vector of the RIS in time slot t and define the user set as $\mathcal{K} = \{1, \dots, K\}$. Assume that users transmit pilot sequences of length τ_k one by one for channel estimation. During the uplink transmission, in time slot t, $1 \le t \le \tau_k$, the received signal from user k at the BS can be expressed as

$$\mathbf{y}_k(t) = \mathbf{H}\mathrm{Diag}\{\mathbf{e}_t\}\mathbf{h}_k\sqrt{p}s_k(t) + \mathbf{n}_k(t),\tag{6}$$

where $s_k(t)$ is the pilot signal of the k-th user, $\mathbf{n}_k(t) \in \mathbb{C}^{N \times 1} \sim \mathcal{CN}(0, \delta^2 \mathbf{I})$ represents additive white Gaussian noise (AWGN) with power δ^2 at the BS when user k is transmitting. The scalar p denotes the transmit power of each user. Assume the pilot symbols satisfy $s_k(t) = 1, 1 \le t \le \tau_k$, so that Eq. (6) can be expressed as

$$\mathbf{y}_k(t) = \mathbf{H}\mathrm{Diag}\{\mathbf{h}_k\}\mathbf{e}_t\sqrt{p} + \mathbf{n}_k(t) \triangleq \mathbf{G}_k\mathbf{e}_t\sqrt{p} + \mathbf{n}_k(t).$$
 (7)

Here, $G_k = HDiag\{h_k\}$ is regarded as the cascaded user-RIS-BS channel of user k, which is the channel to be estimated in this work. Combining (4) and (5), G_k can be rewritten as

$$\mathbf{G}_{k} = \mathbf{A}_{N} \mathbf{\Lambda} \mathbf{A}_{M}^{\mathrm{H}} \mathrm{Diag} \{ \mathbf{A}_{M,k} \boldsymbol{\beta}_{k} \}, \quad \forall k \in \mathcal{K}.$$
 (8)

Stacking the τ_k time slots of (7), the received matrix $\mathbf{Y}_k = [\mathbf{y}_k(1), \dots, \mathbf{y}_k(\tau_k)]$ is given by

$$\mathbf{Y}_k = \sqrt{p} \mathbf{G}_k \mathbf{E}_k + \mathbf{N}_k \in \mathbb{C}^{N \times \tau_k}, \tag{9}$$

where $\mathbf{E}_k = [\mathbf{e}_1, \dots, \mathbf{e}_{\tau_k}] \in \mathbb{C}^{M \times \tau_k}$ can be treated as the phase shift training matrix of the RIS for user k and $\mathbf{N}_k = [\mathbf{n}_k(1), \dots, \mathbf{n}_k(\tau_k)] \in \mathbb{C}^{N \times \tau_k}$.

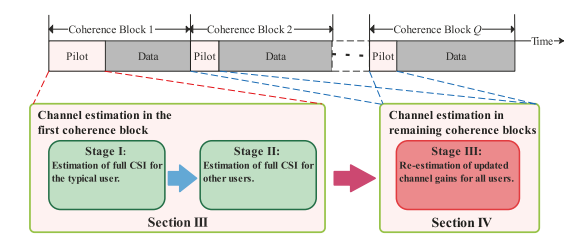


Fig. 1. The proposed three-stage channel estimation protocol.

B. Three-Stage Channel Estimation Protocol

The main idea of the proposed channel estimation protocol are depicted in Fig. 1, where "Pilot" and "Data" represent the phases for uplink channel estimation, and downlink data transmission at the BS side, respectively. Our work focus on the uplink channel estimation of the cascaded channels. Specifically, in Stage I, only one user's cascaded channel is estimated. For convenience, this user is referred to as the typical user.² Information regarding the common RIS-BS channel from the estimate of the typical user's CSI is extracted in order to reduce the pilot overhead of channel estimation for other users in the next stage. Then, in Stage II, the cascaded channel of other users is divided into two parts, a common part and a unique part. The common parts can be readily obtained with the estimated angle information and cascaded gains of the typical user obtained in the first stage. This can help reduce the pilot overhead of estimating the other users' cascaded channel since only a few pilots are required for estimating their unique parts. Finally, it is observed that in the quasistatic situation, the positions of the BS and the RIS are fixed, and the changes in the physical positions of the users and their surrounding obstacles are negligible over milliseconds, corresponding to several channel coherence blocks [25], [26]. This observation leads to the reasonable assumption that the angles remain unchanged for multiple coherence blocks while the gains change from block to block. Hence, Stage III is used for estimating the varying channel gains for all users.

In the following sections, we can conclude that the pilots required for different users depend on the number of paths between the user side and the RIS, which can be estimated by the BS in this work. This needs BS to determine the typical user, allocate the pilot slots required for different users, and inform the users of this knowledge before the next estimation period. The details of the adopted protocol will be discussed later, first for the single-antenna user case and then finally for the multi-antenna user case.

III. ESTIMATION IN THE FIRST COHERENCE BLOCK: STAGE I AND STAGE II

In this section, we start from the single-antenna user case to describe the details of full CSI estimation of all users in the first coherence block, formulating it as two sparse recovery problems in Stage I and Stage II. Then, we analyze the pilot overhead and computational complexity of the proposed method. This section lays the foundation for the extension to the multi-antenna user case in Section V.

A. Stage I: Estimation of Full CSI for Typical User

In this subsection, we provide details on full CSI estimation for a typical single-antenna user, denoted as user 1, where the common AoAs are first estimated and then the cascaded gains and AoDs are obtained.

1) Estimation of Common AoAs: Due to the UPA deployed at the BS and the RIS, the direct DFT approach in [17] and [21] cannot be used for AoA estimation from \mathbf{Y}_1 in (9). Therefore, we propose a modified DFT approach utilizing the properties of the Kronecker product to estimate the common AoAs at the BS of the cascaded channel, i.e., \mathbf{A}_N in (4). To this end, we first provide two lemmas as follows.

Lemma 1: When $N_1 \to \infty$ and $N_2 \to \infty$, the following property holds

$$\lim_{N \to \infty} \frac{1}{N} \mathbf{a}_N^{\mathrm{H}}(\psi_j, \nu_j) \mathbf{a}_N(\psi_i, \nu_i) = \begin{cases} 1 & \psi_j = \psi_i, \nu_i = \nu_j \\ 0 & \textit{otherwise}, \end{cases}$$
(10)

where $N = N_1 \times N_2$. (10) implies that $\mathbf{A}_N^H \mathbf{A}_N = N \mathbf{I}_L$ where \mathbf{I}_L is the identity matrix with dimension $L \times L$.

Proof: Please refer to Appendix A. Define an equivalent Fourier matrix $\widetilde{\mathbf{U}}_N \triangleq \mathbf{U}_{N_1} \otimes \mathbf{U}_{N_2} \in \mathbb{C}^{N \times N}$, where \mathbf{U}_{N_1} and \mathbf{U}_{N_2} are the DFT matrices with (n,m)-th entries $[\mathbf{U}_{N_1}]_{n,m} = \frac{1}{\sqrt{N_1}} e^{-\mathrm{i} \frac{2\pi (n-1)(m-1)}{N_1}}$ and $[\mathbf{U}_{N_2}]_{n,m} = \frac{1}{\sqrt{N_2}} e^{-\mathrm{i} \frac{2\pi (n-1)(m-1)}{N_2}}$, respectively. It can be readily verified that $\widetilde{\mathbf{U}}_N$ is a symmetric and unitary matrix according to its definition. Now we show an asymptotic property of \mathbf{A}_N via the linear transformation $\widetilde{\mathbf{U}}_N^{\mathrm{H}}$.

Lemma 2: When $N_1 \to \infty$ and $N_2 \to \infty$, if the condition $\frac{d_{\rm BS}}{\lambda_c} \leq \frac{1}{2}$ holds,³ then the linear transformation $\widetilde{\mathbf{U}}_N^{\rm H} \mathbf{A}_N$ is a tall sparse matrix with only one nonzero element in each column, i.e.,

$$\lim_{N \to \infty} [\widetilde{\mathbf{U}}_N^{\mathrm{H}} \mathbf{A}_N]_{n_l, l} \neq 0, \quad \forall l, \tag{11}$$

where

$$n_l = (n_1(l) - 1)N_2 + n_2(l),$$
 (12)

and

$$n_{1}(l) = \begin{cases} N_{1}\psi_{l} + 1 & \psi_{l} \in [0, \frac{d_{\text{BS}}}{\lambda_{c}}) \\ N_{1} + N_{1}\psi_{l} + 1 & \psi_{l} \in [-\frac{d_{\text{BS}}}{\lambda_{c}}, 0), \end{cases}$$

$$n_{2}(l) = \begin{cases} N_{2}\nu_{l} + 1 & \nu_{l} \in [0, \frac{d_{\text{BS}}}{\lambda_{c}}) \\ N_{2} + N_{2}\nu_{l} + 1 & \nu_{l} \in [-\frac{d_{\text{BS}}}{\lambda_{c}}, 0). \end{cases}$$
(13)

Proof: Please refer to Appendix B. Since typically $L \ll N_1, N_2$, Lemma 2 means that matrix $\widetilde{\mathbf{U}}_N^{\mathrm{H}} \mathbf{A}_N$ is a row sparse matrix with full column rank. By substituting (8) into (9), we observe that $\widetilde{\mathbf{U}}_N^{\mathrm{H}} \mathbf{Y}_1$ is an asymptotically row-sparse matrix with L nonzero rows, and

²The user closest to the RIS is generally chosen as the typical user since its reflected channel suffers from less severe path loss. Thus, the received signal at the BS is stronger to ensure high estimation performance. The location of users can be obtained using the global position system (GPS) [24], for example.

³This condition holds to avoid AoA ambiguity.

each row corresponds to one of the AoA pairs i.e., (ψ_l, ν_l) . Based on this fact, the estimation of the common AoAs is equivalent to finding the indices of the nonzero rows of $\mathbf{U}_{N}^{\mathrm{H}}\mathbf{Y}_{1}$. Note that $n_{1}(l)$, $n_{2}(l)$ are integers, and can be derived from (12) as follows

$$n_1(l) = \left\lceil \frac{n_l}{N_2} \right\rceil, \ n_2(l) = n_l - N_2(n_1(l) - 1).$$
 (14)

By combining (14) with Lemma 2, the AoA spatial frequency pairs $\{(\psi_l, \nu_l)\}_{l=1}^L$ can be readily estimated. Due to the fact that different scatterers have different angles, we can draw the conclusion that any two nonzero elements are not in the same row, i.e., $n_l \neq n_i$ for any $l \neq i$.

2) Low-Complexity Angle Rotation for Suppressing Power Leakage: To improve the angle estimation accuracy, the power leakage issue [21] should be considered. In practice, finite values for N_1 and N_2 lead to power leakage, which means that the resolution of the estimated AoA (ψ_l, ν_l) is limited by half of the DFT interval, i.e., $\frac{1}{2N_1}$ and $\frac{1}{2N_2}$. To mitigate the power leakage, an angle rotation operation is adopted and the rotation matrix is defined as

$$\mathbf{R}(\Delta\psi, \Delta\nu) = \mathbf{R}_1(\Delta\psi) \otimes \mathbf{R}_2(\Delta\nu), \tag{15}$$

where the diagonal matrices $\mathbf{R}_1(\Delta \psi)$ and $\mathbf{R}_2(\Delta \nu)$ are respectively given by

$$\begin{aligned} \mathbf{R}_{1}(\Delta\psi) &= \mathrm{Diag}\{1, e^{-\mathrm{i}\Delta\psi}, \dots, e^{-\mathrm{i}(N_{1}-1)\Delta\psi}\}, & \text{(16a)} \\ \mathbf{R}_{2}(\Delta\nu) &= \mathrm{Diag}\{1, e^{-\mathrm{i}\Delta\nu}, \dots, e^{-\mathrm{i}(N_{2}-1)\Delta\nu}\}, & \text{(16b)} \end{aligned}$$

where $\Delta\psi\in[-\frac{\pi}{N_1},\frac{\pi}{N_1}]$ and $\Delta\nu\in[-\frac{\pi}{N_2},\frac{\pi}{N_2}]$. We construct L rotation matrices $\mathbf{R}(\Delta\psi_l,\Delta\nu_l)$ to compensate for the Lestimated AoAs (ψ_l, ν_l) . After angle rotation, the central point, denoted as the (n_l, l) -th element of $\mathbf{U}_N^{\mathrm{H}} \mathbf{R}(\Delta \psi_l, \Delta \nu_l) \mathbf{A}_N$, is calculated as

$$\begin{aligned} & [\widetilde{\mathbf{U}}_{N}^{H} \mathbf{R}(\Delta \psi_{l}, \Delta \nu_{l}) \mathbf{A}_{N}]_{n_{l}, l} \\ &= [\mathbf{U}_{N_{1}}^{H} \mathbf{R}_{1}(\Delta \psi_{l}) \mathbf{a}_{N_{1}}(\psi_{l})]_{n_{1}(l)} \otimes [\mathbf{U}_{N_{2}}^{H} \mathbf{R}_{2}(\Delta \nu_{l}) \mathbf{a}_{N_{2}}(\nu_{l}))]_{n_{2}(l)} \\ &= (\sqrt{\frac{1}{N_{1}}} \sum_{m=1}^{N_{1}} e^{-i2\pi(m-1)(\psi_{l} + \frac{\Delta \psi_{l}}{2\pi} - \frac{n_{1}(l) - 1}{N_{1}})}) \\ &\times (\sqrt{\frac{1}{N_{2}}} \sum_{m=1}^{N_{2}} e^{-i2\pi(m-1)(\nu_{l} + \frac{\Delta \nu_{l}}{2\pi} - \frac{n_{2}(l) - 1}{N_{2}})}). \end{aligned}$$
(17)

It can be found that the entries of $\mathbf{U}_N^H \mathbf{R}(\Delta \psi_l, \Delta \nu_l) \mathbf{A}_N$ have only L nonzero elements when

$$\Delta \psi_l = 2\pi \left(\frac{n_1(l) - 1}{N_1} - \psi_l\right), \quad \Delta \nu_l = 2\pi \left(\frac{n_2(l) - 1}{N_2} - \nu_l\right). \tag{18}$$

The $(\Delta \psi_l, \Delta \nu_l)$ in (18) are the required optimal angle rotation parameters for (ψ_l, ν_l) , which concentrates the power of the respective frequency points and suppress power leakage. The optimal angle rotation parameters $(\Delta \psi_l, \Delta \hat{\nu}_l)$ can be found via a 2-D search over the very small region $\Delta \psi_l \in [-\frac{\pi}{N_1}, \frac{\pi}{N_1}]$ and $\Delta\nu_l \in \left[-\frac{\pi}{N_2}, \frac{\pi}{N_2}\right]$ [21], as follows:

$$(\Delta \widehat{\psi}_{l}, \Delta \widehat{\nu}_{l}) = \arg \max_{\Delta \psi_{l} \in [-\frac{\pi}{N_{1}}, \frac{\pi}{N_{1}}], \Delta \nu_{l} \in [-\frac{\pi}{N_{2}}, \frac{\pi}{N_{2}}]} \| \| [\widetilde{\mathbf{U}}_{N}]_{: n_{l}}^{\mathbf{H}} \mathbf{R}(\Delta \psi_{l}, \Delta \nu_{l}) \mathbf{Y}_{1} \|^{2}.$$
(19)

The accuracy of the AoA estimation depends on the number of grid points. The complexity of the 2-D search is approximately $\mathcal{O}(Lg_1g_2)$, where g_1 and g_2 denote the number of grid points in the interval $[-\frac{\pi}{N_1},\frac{\pi}{N_1}]$ and $[-\frac{\pi}{N_2},\frac{\pi}{N_2}]$, respectively. Obviously, large values for g_1 and g_2 lead to high computational complexity. Therefore, we exploit the structure of the steering vector and propose a 1-D search method to reduce the complexity of angle rotation. We note that the first elements of the steering vectors, i.e., $\mathbf{a}_{N_1}(\psi_l)$ or $\mathbf{a}_{N_2}(\nu_l)$, are equal to 1. Using this fact, we can divide the 2-D search into two 1-D searches. Specifically, we construct two rotation matrices shown below to rotate ψ and ν , as

$$\widetilde{\mathbf{R}}_1(\Delta \psi) \triangleq \mathbf{R}_1(\Delta \psi) \otimes \mathbf{D}_{N_2}, \ \widetilde{\mathbf{R}}_2(\Delta \nu) \triangleq \mathbf{D}_{N_1} \otimes \mathbf{R}_2(\Delta \nu), \ (20)$$

where $\mathbf{R}_1(\Delta \psi)$ and $\mathbf{R}_2(\Delta \nu)$ are defined in (16). The matrices $\mathbf{D}_{N_1} \in \mathbb{C}^{N_1 \times N_1}$ and $\mathbf{D}_{N_2} \in \mathbb{C}^{N_2 \times N_2}$ are diagonal whose (1,1) entry is equal to 1 and whose other elements are 0. Defining $\widetilde{\mathbf{U}}_1 \triangleq \mathbf{U}_{N_1} \otimes \mathbf{D}_{N_2}$ and $\widetilde{\mathbf{U}}_2 \triangleq \mathbf{D}_{N_1} \otimes \mathbf{U}_{N_2}$, we have the following proposition.

Proposition 1: The angle estimation operation for the l-th AoA pair (ψ_l, ν_l) shown in (17) can be divided into two independent angle rotation operations with the $(\overline{n_{1l}}, l)$ th element of $\widetilde{\mathbf{U}}_{1}^{\mathrm{H}}\widetilde{\mathbf{R}}_{1}(\Delta\psi_{l})\mathbf{A}_{N}$, and the $(\overline{n_{2l}},l)$ -th element of $\widetilde{\mathbf{U}}_{2}^{\mathrm{H}}\widetilde{\mathbf{R}}_{2}(\Delta\nu_{l})\mathbf{A}_{N}$, where $\overline{n_{1l}}$ and $\overline{n_{2l}}$ denote the nonzero element of the l-th column of $\mathbf{U}_1^{\mathrm{H}}\mathbf{R}_1(\Delta\psi_l)\mathbf{A}_N$ and $\widetilde{\mathbf{U}}_{2}^{\mathrm{H}}\widetilde{\mathbf{R}}_{2}(\Delta\nu_{l})\mathbf{A}_{N}$, respectively, and satisfy

$$\overline{n_{1l}} = (n_1(l) - 1)N_2 + 1, \quad \overline{n_{2l}} = n_2(l).$$
 (21)

Proof: Please refer to Appendix C. Based on Proposition 1, the optimal angle rotation parameters $(\Delta \psi_l, \Delta \widehat{\nu}_l)$ for (ψ_l, ν_l) can be found by solving the two separate 1-D search problems shown in (22), which significantly reduces the complexity to $\mathcal{O}(L(q_1+q_2))$:

$$\Delta \widehat{\psi}_l = \arg \max_{\Delta \psi_l \in [-\frac{\pi}{N_1}, \frac{\pi}{N_1}]} ||[\widetilde{\mathbf{U}}_1]_{:,\overline{n_{1l}}}^{\mathbf{H}} \widetilde{\mathbf{R}}_1(\Delta \psi_l) \mathbf{Y}_1||^2, \quad (22a)$$

$$\Delta \widehat{\nu}_{l} = \arg \max_{\Delta \nu_{l} \in [-\frac{\pi}{N_{2}}, \frac{\pi}{N_{2}}]} ||[\widetilde{\mathbf{U}}_{2}]_{:,\overline{n_{2}l}}^{\mathbf{H}} \widetilde{\mathbf{R}}_{2}(\Delta \nu_{l}) \mathbf{Y}_{1}||^{2}.$$
 (22b)

Denote the estimated angle rotations as $\{(\Delta \hat{\psi}_l, \Delta \hat{\nu}_l)\}_{l=1}^L$, then the estimated AoA spatial frequency pair of the l-th path is given by

$$\hat{\psi}_{l} = \begin{cases} \frac{n_{1}(l) - 1}{N_{1}} - \frac{\Delta \hat{\psi}_{l}}{2\pi} & n_{1}(l) \leq N_{1} \frac{d_{\text{BS}}}{\lambda_{c}} \\ \frac{n_{1}(l) - 1}{N_{1}} - 1 - \frac{\Delta \hat{\psi}_{l}}{2\pi} & n_{1}(l) > N_{1} \frac{d_{\text{BS}}}{\lambda_{c}}, \end{cases}$$
(23a)

$$\hat{\nu}_{l} = \begin{cases}
\frac{n_{2}(l) - 1}{N_{2}} - \frac{\Delta \hat{\nu}_{l}}{2\pi} & n_{2}(l) \leq N_{2} \frac{d_{\text{BS}}}{\lambda_{c}} \\
\frac{n_{2}(l) - 1}{N_{2}} - 1 - \frac{\Delta \hat{\nu}_{l}}{2\pi} & n_{2}(l) > N_{2} \frac{d_{\text{BS}}}{\lambda_{c}}.
\end{cases} (23b)$$

With the estimated spatial frequency pairs for the AoAs, $\{(\hat{\psi}_l, \hat{\nu}_l)\}_{l=1}^L$, we can obtain an estimate of the common AoA steering matrix $\widehat{\mathbf{A}}_N = [\mathbf{a}_N(\widehat{\psi}_1, \widehat{\nu}_1), \dots, \mathbf{a}_N(\widehat{\psi}_{\widehat{L}}, \widehat{\nu}_{\widehat{L}})] \in$ $\mathbb{C}^{N \times \widehat{L}}$. AoA estimation of the different paths at the BS is summarized in Algorithm 1, where $\Gamma(\mathbf{z})$ represents the $||[\widetilde{\mathbf{U}}_N]_{l=n}^{\mathrm{H}} \mathbf{R}(\Delta \psi_l, \Delta \nu_l) \mathbf{Y}_1||^2$. (19) operation of searching the peak power of vector \mathbf{z} and \widehat{L} is the estimated number of propagation paths in step 3.⁴ Ω_N , Ω_{N_1} , and Ω_{N_2} are the sets with cardinality \widehat{L} , and denote the position indices of the nonzero rows for $\widetilde{\mathbf{U}}_N^{\mathrm{H}} \mathbf{A}_N$, $\mathbf{U}_{N_1}^{\mathrm{H}} \mathbf{A}_{N_1}$, and $\mathbf{U}_{N_2}^{\mathrm{H}} \mathbf{A}_{N_2}$, respectively.

Algorithm 1 Low-Complexity Angle Rotation Based AoA Estimation

Input: Y_1 .

- 1: Calculate linear transformation of \mathbf{Y}_1 : $\widetilde{\mathbf{Y}}_1 = \widetilde{\mathbf{U}}_N^{\mathrm{H}} \mathbf{Y}_1$;
- 2: Calculate the sum power of each row: $\mathbf{z}(n) = ||[\widetilde{\mathbf{Y}}_1]_{n,:}||^2, \forall n = 1, 2, \dots, N;$
- 3: Find the rows with the peak power: $(\Omega_N, \widehat{L}) = \Gamma(\mathbf{z})$, where $\Omega_N = \{n_l, l = 1, \dots, \widehat{L}\}$;
- 4: Construct two sets: $\Omega_{N_1} = \{n_1(l), l = 1, \dots, \widehat{L}\}, \Omega_{N_2} = \{n_2(l), l = 1, \dots, \widehat{L}\}$ via (14);
- 5: for $1 \leq l \leq \widehat{L}$ do
- 6: Calculate $\overline{n_{1l}}$ and $\overline{n_{2l}}$ respectively via (21);
- 7: Find $\Delta \psi_l$ and $\Delta \widehat{\nu}_l$ via (22);
- 8: Estimate ψ_l and $\widehat{\nu}_l$ according to (23);
- 9: end for

Output: $\{(\widehat{\psi}_l, \widehat{\nu}_l)\}_{l=1}^{\widehat{L}}$ and $\widehat{\mathbf{A}}_N$.

Remark 1: Since the common AoA steering matrix \mathbf{A}_N is shared by all users in MU scenario, the received signals from K users in Stage I and Stage II during the first coherence block can be utilized jointly to estimate \mathbf{A}_N . Accordingly, the input of Algorithm 1 is given by $\mathbf{Y} = [\mathbf{Y}_1, \mathbf{Y}_2, \dots, \mathbf{Y}_K] \in \mathbb{C}^{N \times (\sum_{k=1}^K \tau_k)}$. In this case, the number of measurements used for the estimation of \mathbf{A}_N increases, which enhances the estimation performance and alleviates the error propagation effect in the following stages.

3) Estimation of the Cascaded Spatial Frequencies and Gains: By substituting $\mathbf{A}_N = \widehat{\mathbf{A}}_N + \Delta \mathbf{A}_N$ and applying Lemma 1, we take the linear transformation $\frac{1}{N\sqrt{p}}\widehat{\mathbf{A}}_N^{\mathrm{H}}$ of the received signals to eliminate the effects of the common AoAs, i.e.,

$$\frac{1}{N\sqrt{p}}\widehat{\mathbf{A}}_{N}^{\mathrm{H}}\mathbf{Y}_{1} = \mathbf{\Lambda}\mathbf{A}_{M}^{\mathrm{H}}\mathrm{Diag}\{\mathbf{h}_{1}\}\mathbf{E}_{1} + \frac{1}{N\sqrt{p}}\widehat{\mathbf{A}}_{N}^{\mathrm{H}}(\mathbf{N}_{1} + \sqrt{p}\Delta\mathbf{A}_{N}\mathbf{\Lambda}\mathbf{A}_{M}^{\mathrm{H}}\mathrm{Diag}\{\mathbf{h}_{1}\}\mathbf{E}_{1}).$$
(24)

Here, $\Delta \mathbf{A}_N \triangleq \mathbf{A}_N - \widehat{\mathbf{A}}_N$ is treated as the estimation error between the common AoA and its estimate, and the third term $(\frac{1}{N}\widehat{\mathbf{A}}_N^H \Delta \mathbf{A}_N \mathbf{\Lambda} \mathbf{A}_M^H \mathrm{Diag}\{\mathbf{h}_1\}\mathbf{E}_1)$ represents the corresponding negative error propagation effect. Clearly, $\Delta \mathbf{A}_N$ can be reduced effectively via the MU joint estimation strategy discussed in Remark 1.

Now we define the transpose of $\frac{1}{N\sqrt{p}}\widehat{\mathbf{A}}_N^{\mathrm{H}}\mathbf{Y}_1$ as an equivalent measurement matrix $\overline{\mathbf{Y}}_1 \in \mathbb{C}^{\tau_1 \times L}$ shown below

$$\overline{\mathbf{Y}}_{1} \triangleq \left(\frac{1}{N\sqrt{p}}\widehat{\mathbf{A}}_{N}^{\mathrm{H}}\mathbf{Y}_{1}\right)^{\mathrm{H}} \\
= \mathbf{E}_{1}^{\mathrm{H}}\mathrm{Diag}\{\mathbf{h}_{1}^{*}\}\mathbf{A}_{M}\mathbf{\Lambda}^{*} + \overline{\mathbf{N}}_{1} = \mathbf{E}_{1}^{\mathrm{H}}\mathbf{H}_{\mathrm{RIS}} + \overline{\mathbf{N}}_{1}, \quad (25)$$

⁴If the power of the row is lager than that of its neighbor rows, and far exceeds the minimum power of $\mathbf{z}(n)$ based on a adjustable predefined ratio threshold, we put this row index into set Ω_N . Alternately, classical minimum description length (MDL) and novel signal subspace matching (SSM) schemes [27] can be adopted as a pre-processing operation before Algorithm 1 to determine the \hat{L} .

where $\mathbf{H}_{RIS} \triangleq \operatorname{Diag}\{\mathbf{h}_{1}^{*}\}\mathbf{A}_{M}\mathbf{\Lambda}^{*}$ and $\overline{\mathbf{N}}_{1}$ is the corresponding transpose of the second term in Eq. (24), seen as the equivalent noise. By exploiting the structure of \mathbf{H}_{RIS} , we have

$$\mathbf{H}_{\mathrm{RIS}} = \mathbf{h}_{1}^{*} \bullet (\mathbf{A}_{M} \mathbf{\Lambda}^{*}) = (\mathbf{A}_{M,1} \boldsymbol{\beta}_{1})^{*} \bullet (\mathbf{A}_{M} \mathbf{\Lambda}^{*})$$
$$= (\mathbf{A}_{M,1}^{*} \bullet \mathbf{A}_{M})(\boldsymbol{\beta}_{1}^{*} \otimes \mathbf{\Lambda}^{*}), \tag{26}$$

where $\mathbf{A}_{M,1}^* \bullet \mathbf{A}_M = [\mathbf{a}_M(\omega_1 - \varphi_{1,1}, \mu_1 - \theta_{1,1}), \mathbf{a}_M(\omega_2 - \varphi_{1,1}, \mu_2 - \theta_{1,1}) \dots, \mathbf{a}_M(\omega_L - \varphi_{1,J_1}, \mu_L - \theta_{1,J_1})] \in \mathbb{C}^{M \times J_1 L}$, and the last equality uses the identity $(\mathbf{A} \bullet \mathbf{B})(\mathbf{C} \otimes \mathbf{D}) = (\mathbf{A}\mathbf{C}) \bullet (\mathbf{B}\mathbf{D})$ [28]. To extract the cascaded directional spatial frequency pairs $\{(\omega_l - \varphi_{1,j}, \mu_l - \theta_{1,j})\}_{j=1,l=1}^{J_1 L}$ and gains $(\beta_1^* \otimes \mathbf{\Lambda}^*)$ from $\overline{\mathbf{Y}}_1$, (25) could be approximated using the virtual angular domain (VAD) representation and converted into a J_1L -sparse recovery problem via vectorization [13], but this approach has high complexity and performance loss.

Instead, another method is developed as follows. We first estimate J_1 cascaded spatial frequency pairs and gains from a typical column vector of $\overline{\mathbf{Y}}_1$ using CS, and then estimate the remaining parameters by exploiting the correlation between the typical column and other columns. Specifically, denote $\overline{\mathbf{y}}_r$ as the r-th column of $\overline{\mathbf{Y}}_1$, which is given by

$$\overline{\mathbf{y}}_{r} = \mathbf{E}_{1}^{\mathrm{H}} \mathrm{Diag}\{\mathbf{h}_{1}^{*}\}[\mathbf{A}_{M}\boldsymbol{\Lambda}^{*}]_{:,r} + \overline{\mathbf{n}}_{r} \\
= \mathbf{E}_{1}^{\mathrm{H}} \mathbf{h}_{1}^{*} \bullet (\alpha_{r}^{*} \mathbf{a}_{M}(\omega_{r}, \mu_{r})) + \overline{\mathbf{n}}_{r} \\
= \mathbf{E}_{1}^{\mathrm{H}} (\mathbf{A}_{M,1}^{*} \bullet \mathbf{a}_{M}(\omega_{r}, \mu_{r})) \alpha_{r}^{*} \boldsymbol{\beta}_{1}^{*} + \overline{\mathbf{n}}_{r}, \tag{27}$$

where $\mathbf{A}_{M,1}^* \bullet \mathbf{a}_M(\omega_r, \mu_r) = [\mathbf{a}_M(\omega_r - \varphi_{1,1}, \mu_r - \theta_{1,1}), \dots, \mathbf{a}_M(\omega_r - \varphi_{1,J_1}, \mu_r - \theta_{1,J_1})] \in \mathbb{C}^{M \times J_1}$ and $\overline{\mathbf{n}}_r$ is the r-th column of $\overline{\mathbf{N}}_1$. Note that $\mathrm{Diag}\{\mathbf{h}_1^*\}[\mathbf{A}_M \boldsymbol{\Lambda}^*]_{:,r}$ is the r-th column of $\mathbf{H}_{\mathrm{RIS}}$, which we denote as $\mathbf{h}_{\mathrm{RIS},r}$. Since $\{(\omega_r - \varphi_{1,j})\}_{j=1}^{J_1}$ and $\{(\mu_r - \theta_{1,j})\}_{j=1}^{J_1}$ lie in the interval $[-2\frac{d_{\mathrm{RIS}}}{\lambda_c}, 2\frac{d_{\mathrm{RIS}}}{\lambda_c}]$, we can formulate (27) as a J_1 -sparse signal recovery problem

$$\overline{\mathbf{y}}_r = \mathbf{E}_1^{\mathrm{H}} (\mathbf{A}_1 \otimes \mathbf{A}_2) \mathbf{b}_r + \overline{\mathbf{n}}_r, \tag{28}$$

where $\mathbf{A}_1 \in \mathbb{C}^{M_1 \times D_1}$ and $\mathbf{A}_2 \in \mathbb{C}^{M_2 \times D_2}$ are overcomplete dictionary matrices $(D_1 \geq M_1, D_2 \geq M_2)$ with resolutions $\frac{1}{D_1}$ and $\frac{1}{D_2}$, respectively, and the columns of \mathbf{A}_1 and \mathbf{A}_2 contain values for $\mathbf{a}_{M_1}(\omega_r - \varphi_{1,j})$ and $\mathbf{a}_{M_2}(\mu_r - \theta_{1,j})$ on the angle grid, i.e., $\mathbf{A}_1 = [\mathbf{a}_{M_1}(-2\frac{d_{\mathrm{RIS}}}{\lambda_c}), \mathbf{a}_{M_1}((-2+\frac{4}{D_1})\frac{d_{\mathrm{RIS}}}{\lambda_c}), \ldots, \mathbf{a}_{M_1}((2-\frac{4}{D_1})\frac{d_{\mathrm{RIS}}}{\lambda_c})]$ and $\mathbf{A}_2 = [\mathbf{a}_{M_2}(-2\frac{d_{\mathrm{RIS}}}{\lambda_c}), \mathbf{a}_{M_2}((-2+\frac{4}{D_2})\frac{d_{\mathrm{RIS}}}{\lambda_c}), \ldots, \mathbf{a}_{M_2}((2-\frac{4}{D_2})\frac{d_{\mathrm{RIS}}}{\lambda_c})]$.

In addition, $\mathbf{b}_r \in \mathbb{C}^{D_1D_2 \times 1}$ in (28) is a sparse vector with J_1 nonzero entries corresponding to the cascaded channel path gains $\{\alpha_r^*\beta_{1,j}^*\}_{j=1}^{J_1}$. To obtain the best possible CS performance, the RIS phase shift training matrix \mathbf{E}_1 should be designed to ensure that the columns of the equivalent dictionary $\mathbf{E}_1^{\mathrm{H}}(\mathbf{A}_1 \otimes \mathbf{A}_2)$ are orthogonal. A detailed design of \mathbf{E}_1 that achieves this goal can be found in [17]. A simpler method is to choose the random Bernoulli matrix as \mathbf{E}_1 , i.e., randomly generate the elements of \mathbf{E}_1 from $\{-1, +1\}$ with equal probability [16]. Later in Section VI, we will show

that this random method has near-optimal performance, and provides a nearly orthogonal equivalent dictionary.⁵

Using CS, we obtain the cascaded AoD pair, i.e., $(\omega_r-\varphi_{1,j},\mu_r-\theta_{1,j})$. The corresponding cascaded AoD, i.e., $(\omega_r-\varphi_{1,j})$ and $(\mu_r-\theta_{1,j})$, can be obtained similarly using the properties of the Kronecker product. Assume that the m-th element of sparse vector \mathbf{b}_r is nonzero, then the m-th column of $(\mathbf{A}_1\otimes\mathbf{A}_2)$ is the corresponding cascaded steering vector. The corresponding indices in \mathbf{A}_1 and \mathbf{A}_2 , denoted as m_1 and m_2 , can be derived as

$$m_1 = \left\lceil \frac{m}{D_2} \right\rceil, \ m_2 = m - D_2(m_1 - 1).$$
 (29)

Finally, we obtain the estimate of the cascaded AoD, i.e., $\{(\widehat{\omega_r-\varphi_{1,j}})\}_{j=1}^{\hat{J}_1}$ and $\{(\widehat{\mu_r-\theta_{1,j}})\}_{j=1}^{\hat{J}_1}$. As a result, $\widehat{\mathbf{h}}_{\mathrm{RIS},r}$ is obtained according to (27). Estimates of the other columns of $\mathbf{H}_{\mathrm{RIS}}$, i.e., $\{\mathbf{h}_{\mathrm{RIS},l}\}_{l\neq r}^L$, can be obtained by exploiting the correlation among different columns. To illustrate the correlation relationship, a compensation matrix $\Delta\mathbf{H}_l$ with respect to the reference index r is defined as

$$\Delta \mathbf{H}_{l} = \frac{\alpha_{l}^{*}}{\alpha_{r}^{*}} \operatorname{Diag}\{\mathbf{a}_{M}(\omega_{l} - \omega_{r}, \mu_{l} - \mu_{r})\}$$
$$= \gamma_{l} \operatorname{Diag}\{\mathbf{a}_{M}(\Delta \omega_{l}, \Delta \mu_{l})\}, \tag{30}$$

where $\Delta\omega_l$, $\Delta\mu_l$ are rotation factors and γ_l is a gain scaling factor given by

$$\Delta\omega_l = \omega_l - \omega_r, \quad \Delta\mu_l = \mu_l - \mu_r, \quad \gamma_l = \frac{\alpha_l^*}{\alpha_r^*}.$$
 (31)

Clearly, $\Delta\omega_l$, $\Delta\mu_l \in \left[-2\frac{d_{\rm RIS}}{\lambda_c}, 2\frac{d_{\rm RIS}}{\lambda_c}\right]$. Then, we have

 $\Delta \mathbf{H}_l \mathbf{h}_{\mathrm{RIS},r}$

- $= \Delta \mathbf{H}_l \operatorname{Diag}\{\mathbf{h}_1^*\}(\alpha_r^* \mathbf{a}_M(\omega_r, \mu_r))$
- $= \Delta \mathbf{H}_l \operatorname{Diag} \{ \mathbf{a}_M(\omega_r, \mu_r) \} (\alpha_r^* \mathbf{h}_1^*)$
- $= \gamma_l \operatorname{Diag}\{\mathbf{a}_M(\Delta\omega_l, \Delta\mu_l)\} \operatorname{Diag}\{\mathbf{a}_{M_1}(\omega_r) \otimes \mathbf{a}_{M_2}(\mu_r)\} (\alpha_r^* \mathbf{h}_1^*)$
- = $(\text{Diag}\{\mathbf{a}_{M_1}(\Delta\omega_l)\}\text{Diag}\{\mathbf{a}_{M_1}(\omega_r)\})$
 - $\otimes (\operatorname{Diag}\{\mathbf{a}_{M_2}(\Delta\mu_l)\}\operatorname{Diag}\{\mathbf{a}_{M_2}(\mu_r)\})(\alpha_l^*\mathbf{h}_1^*)$
- = $\operatorname{Diag}\{\mathbf{a}_{M_1}(\omega_l)\} \otimes \operatorname{Diag}\{\mathbf{a}_{M_2}(\mu_l)\}(\alpha_l^*\mathbf{h}_1^*) = \mathbf{h}_{\operatorname{RIS},l}.$

This equality shows that we can estimate the compensation matrix $\Delta \mathbf{H}_l$ instead of directly estimating $\mathbf{h}_{\mathrm{RIS},l}$. Specifically, $\mathbf{h}_{\mathrm{RIS},r}$ is estimated by applying CS to (28), and $\mathbf{h}_{\mathrm{RIS},l}$ can be rewritten as

$$\mathbf{h}_{\mathrm{RIS},l} = \gamma_l \mathrm{Diag} \{ \mathbf{a}_M (\Delta \omega_l, \Delta \mu_l) \} \mathbf{h}_{\mathrm{RIS},r}$$

$$= \mathrm{Diag} \{ \mathbf{h}_{\mathrm{RIS},r} \} \mathbf{a}_M (\Delta \omega_l, \Delta \mu_l) \gamma_l. \tag{32}$$

We define $\mathbf{c}_l(\Delta\omega_l, \Delta\mu_l) = \mathbf{E}_1^H \mathrm{Diag}\{\widehat{\mathbf{h}}_{\mathrm{RIS},r}\} \mathbf{a}_M(\Delta\omega_l, \Delta\mu_l)$. Then, by replacing $\mathbf{h}_{\mathrm{RIS},r}$ with $\widehat{\mathbf{h}}_{\mathrm{RIS},r} + \Delta\mathbf{h}_{\mathrm{RIS},r}$, the l-th column of $\overline{\mathbf{Y}}_1$ in (25) is given by

$$\overline{\mathbf{y}}_{l} = \mathbf{E}_{1}^{\mathrm{H}} \mathrm{Diag}\{\mathbf{h}_{\mathrm{RIS},r}\} \mathbf{a}_{M}(\Delta \omega_{l}, \Delta \mu_{l}) \gamma_{l} + \overline{\mathbf{n}}_{l}$$

$$= \mathbf{E}_{1}^{\mathrm{H}} \mathrm{Diag}\{\widehat{\mathbf{h}}_{\mathrm{RIS},r}\} \mathbf{a}_{M}(\Delta \omega_{l}, \Delta \mu_{l}) + \mathbf{n}_{\mathrm{noise}}, \quad (33)$$

where $\mathbf{n}_{\text{noise}} \triangleq \mathbf{E}_{1}^{\text{H}} \text{Diag}\{\Delta \mathbf{h}_{\text{RIS},r}\} \mathbf{a}_{M}(\Delta \omega_{l}, \Delta \mu_{l}) + \overline{\mathbf{n}}_{l}$ represents the corresponding noise vector and $\Delta \mathbf{h}_{\text{RIS},r}$ is the estimation error of $\mathbf{h}_{\text{RIS},r}$.

To find the optimal rotation factors $(\Delta\omega_l, \Delta\mu_l)$, a simple 2-D search method can be used:

$$(\Delta \widehat{\omega}_{l}, \Delta \widehat{\mu}_{l}) = \arg \max_{\Delta \omega, \Delta \mu \in [-2\frac{d_{\text{RIS}}}{\lambda_{c}}, 2\frac{d_{\text{RIS}}}{\lambda_{c}}]} |\langle \overline{\mathbf{y}}_{l}, \mathbf{c}_{l}(\Delta \omega, \Delta \mu) \rangle|.$$
(34)

The gain scaling factor γ_l can be determined as the solution to the least square (LS) problem

$$\widehat{\gamma}_{l} = \arg\min_{x} ||\overline{\mathbf{y}}_{l} - \mathbf{c}_{l}(\Delta\widehat{\omega}_{l}, \Delta\widehat{\mu}_{l})x||, \tag{35}$$

whose solution is $\widehat{\gamma}_l = (\mathbf{c}_l^{\mathrm{H}}(\Delta \widehat{\omega}_l, \Delta \widehat{\mu}_l)\mathbf{c}_l(\Delta \widehat{\omega}_l, \Delta \widehat{\mu}_l))^{-1}$ $\mathbf{c}_l^{\mathrm{H}}(\Delta \widehat{\omega}_l, \Delta \widehat{\mu}_l)\overline{\mathbf{y}}_l$. Substituting the solutions of (34) and (35) into (32), we can obtain $\widehat{\mathbf{h}}_{\mathrm{RIS},l}$, $(1 \leq l \leq L, l \neq r)$. Finally, the estimated cascaded channel of user 1 is given by

$$\widehat{\mathbf{G}}_1 = \widehat{\mathbf{A}}_N \widehat{\mathbf{H}}_{\mathrm{RIS}}^{\mathrm{H}},\tag{36}$$

where $\hat{\mathbf{H}}_{RIS} = [\hat{\mathbf{h}}_{RIS,1}, \cdots, \hat{\mathbf{h}}_{RIS,L}]$. Furthermore, the cascaded AoD in $\mathbf{h}_{RIS,L}$ can be obtained as

$$\omega_l - \varphi_{1,j} = (\omega_r - \varphi_{1,j}) + \Delta\omega_l, \mu_l - \theta_{1,j} = (\mu_r - \theta_{1,j}) + \Delta\mu_l,$$
(37)

where the estimate of $(\omega_r - \varphi_{1,j}, \mu_r - \theta_{1,j})$ and $(\Delta \omega_l, \Delta \mu_l)$ can be readily obtained from (27) and (34), respectively. The overall estimation of G_1 is summarized in Algorithm 2.

Algorithm 2 Estimation of Full CSI for Typical User **Input:** Y₁.

- 1: Return the estimated number of paths between BS and RIS \widehat{L} and AoA steering matrix $\widehat{\mathbf{A}}_N$ from Algorithm 1;
- 2: Calculate equivalent measurement matrix $\overline{\mathbf{Y}}_1 = [\overline{\mathbf{y}}_1, \dots, \overline{\mathbf{y}}_{\widehat{L}}];$
- 3: Choose the typical reference index r and estimate $\mathbf{h}_{RIS,r}$ by solving sparse recovery problem associated with (28);
- 4: **for** $1 \le l \le L, l \ne r$ **do**
- 5: Estimate $(\Delta\omega_l, \Delta\mu_l)$ according to (34);
- 6: Estimate γ_l according to (35);
- 7: Estimate $h_{RIS,l}$ according to (32);

8: end for

Output:
$$\widehat{\mathbf{G}}_1 = \widehat{\mathbf{A}}_N[\widehat{\mathbf{h}}_{RIS,1},\cdots,\widehat{\mathbf{h}}_{RIS,\widehat{L}}]^H$$
.

⁵Please note that the number of scatterers in the user 1-RIS channel, i.e., the sparsity level for the sparse recovery problem associated with (28), denoted as J_1 , is estimated via the selected CS-based techniques. For example, in Section VI, the proposed estimation protocol adopts OMP as the recovery algorithm. In this case, the stopping criteria for this algorithm is based on the power of the residual error, i.e., the algorithm is stopped when the residual energy is smaller than a predefined threshold. Thus the number of iterations is treated as the estimate of J_1 .

 $^{^6\}text{To}$ reduce the error propagation, the reference index r can be chosen based on the maximum received power criterion, i.e., $r = \arg\max_{i \in [1,\widehat{L}]} ||\overline{\mathbf{y}}_i||^2.$

B. Stage II: Estimation of Full CSI for Other Users

In this subsection, the property that all users share the common RIS-BS channel is invoked for reducing the pilot overhead of channel estimation. First, we re-exploit the structure of the cascaded channel \mathbf{G}_k , and then divide it into two parts, i.e., a common part and a unique part. Then, only re-estimating the unique part is necessary for obtaining the full CSI of the other users.

1) Re-Express Cascaded Channel: In order to illustrate the necessity of re-expressing cascaded channel \mathbf{G}_k , let us recall its structure and see why the common RIS-BS channel \mathbf{H} cannot be obtained in Stage I. According to (8), all users share the common \mathbf{H} consisting of three matrices, i.e., \mathbf{A}_N , $\mathbf{\Lambda}$ and \mathbf{A}_M . The first, \mathbf{A}_N , is estimated in Stage I. However, $\mathbf{\Lambda}$ and \mathbf{A}_M cannot be extracted separately from \mathbf{G}_1 since we can only estimate the spatial frequencies of the cascaded AoDs, i.e., $(\omega_l - \varphi_{1,j})$, $(\mu_l - \theta_{1,j})$ and the cascaded gains, i.e., $\alpha_l \beta_{1,j}$ for any l and j. If other users only utilize the obtained $\hat{\mathbf{A}}_N$, the estimation for these users is the same as that of the typical user, and thus the pilot overhead cannot be decreased further. Therefore, we aim to fully exploit the structure of \mathbf{H} so as to utilize the common channel's information from $\mathbf{\Lambda}$ and \mathbf{A}_M .

Motivated by this, we decompose the cascaded channel \mathbf{G}_k into two parts, i.e., a common part and a unique part, where the common part can be obtained from the estimation of \mathbf{G}_1 in Stage I. The constructed common part has the full information of \mathbf{A}_N , and the re-parameterized information of $\mathbf{\Lambda}$ and \mathbf{A}_M , so as to achieve the full exploitation of \mathbf{H} . Then, we only need to re-estimate the unique part of the cascaded channel for the other users. To this end, we denote the common part of \mathbf{G}_k as $\mathbf{H}_s \in \mathbb{C}^{N \times M}$, which can be regarded as a substitute for \mathbf{H} from \mathbf{G}_1 . Similarly, the unique part of \mathbf{G}_k is denoted by $\mathbf{h}_{s,k} \in \mathbb{C}^{M \times 1}$, which can be regarded as a substitute for \mathbf{h}_k . Then, \mathbf{G}_k can be re-expressed as

$$\mathbf{G}_k = \mathbf{H}_{\mathrm{s}} \mathrm{Diag}\{\mathbf{h}_{\mathrm{s},k}\} \in \mathbb{C}^{N \times M}, \quad \forall k \in \mathcal{K}.$$
 (38)

In the following, we first construct the common part \mathbf{H}_s with the knowledge obtained in Stage I. Then, we estimate each user's unique part $\mathbf{h}_{s,k}$.

2) Construction of Common Part: Define the average value of user 1's complex gains β_1 as $\overline{\beta} = \frac{1}{J_1} \mathbf{1}_{J_1}^{\mathrm{T}} \beta_1$, then we have

$$\mathbf{\Lambda} = \operatorname{Diag}\{\alpha_1, \alpha_2, \dots, \alpha_L\} = \alpha_r \operatorname{Diag}\{\gamma_1^*, \gamma_2^*, \dots, \gamma_L^*\}
= \frac{1}{\overline{\beta}} \overline{\beta} \alpha_r \operatorname{Diag}\{\gamma_1^*, \gamma_2^*, \dots, \gamma_L^*\} \triangleq \frac{1}{\overline{\beta}} \mathbf{\Lambda}_{s}.$$
(39)

Here, $\Lambda_s = (\frac{1}{J_1} \mathbf{1}_{J_1}^T \boldsymbol{\beta}_1 \alpha_r) \text{Diag}\{\gamma_1^*, \gamma_2^*, \dots, \gamma_L^*\}$. Obviously, $\boldsymbol{\beta}_1 \alpha_r$ can be obtained by solving the sparse recovery problem corresponding to (27) and γ_l can be obtained according to (35). Thus, the constructed matrix, Λ_s , can be readily calculated.

Similarly, the matrix A_M can be rewritten as

$$\mathbf{A}_{M} = [\mathbf{a}_{M}(\omega_{1}, \mu_{1}), \dots, \mathbf{a}_{M}(\omega_{L}, \mu_{L})]$$

$$= \operatorname{Diag}\{\mathbf{a}_{M}(\omega_{r}, \mu_{r})\}\mathbf{A}_{\Delta M}, \tag{40}$$

where $\mathbf{A}_{\Delta M} = [\mathbf{a}_M(\Delta\omega_1, \Delta\mu_1), \dots, \mathbf{a}_M(\Delta\omega_L, \Delta\mu_L)]$. Note that the rotation factors $\Delta\omega_l$, $\Delta\mu_l$ can be obtained by Algorithm 2, but we need to find (ω_r, μ_r) , which is not possible.

Instead, we introduce two parameters, $\omega_{\rm s}=\frac{1}{J_1}\sum_{j=1}^{J_1}(\omega_r-\varphi_{1,j})$ and $\mu_{\rm s}=\frac{1}{J_1}\sum_{j=1}^{J_1}(\mu_r-\theta_{1,j})$ as substitutes for ω_r and μ_r , which can be readily obtained since $(\omega_r-\varphi_{1,j})$ and $(\mu_r-\theta_{1,j})$ for $\forall j\in\{1,\ldots,J_1\}$ have been estimated in Algorithm 2.

Then, define $\overline{\varphi_1}$ as $(-\frac{1}{J_1}\sum_{j=1}^{J_1}\varphi_{1,j})$ and $\overline{\theta_1}$ as $(-\frac{1}{J_1}\sum_{j=1}^{J_1}\theta_{1,j})$. The following relationship exists between $(\omega_{\rm s},\mu_{\rm s})$ and (ω_r,μ_r) :

$$\omega_{\rm s} = \frac{1}{J_1} \sum_{i=1}^{J_1} (\omega_r - \varphi_{1,i}) = \omega_r + \overline{\varphi_1}, \tag{41a}$$

$$\mu_{\rm s} = \frac{1}{J_1} \sum_{i=1}^{J_1} (\mu_r - \theta_{1,j}) = \mu_r + \overline{\theta_1}.$$
(41b)

Based on the above definitions, $\operatorname{Diag}\{\mathbf{a}_M(\omega_r,\mu_r)\}$ in (40) can be represented as

$$\begin{aligned} \operatorname{Diag} &\{\mathbf{a}_{M}(\omega_{r}, \mu_{r})\} \\ &= \operatorname{Diag} &\{\mathbf{a}_{M}(\omega_{s} - \overline{\varphi_{1}}, \mu_{s} - \overline{\theta_{1}})\} \\ &= \operatorname{Diag} &\{\mathbf{a}_{M_{1}}(\omega_{s} - \overline{\varphi_{1}}) \otimes \mathbf{a}_{M_{2}}(\mu_{s} - \overline{\theta_{1}})\} \\ &= &(\operatorname{Diag} &\{\mathbf{a}_{M_{1}}(-\overline{\varphi_{1}})\} \otimes \operatorname{Diag} &\{\mathbf{a}_{M_{2}}(-\overline{\theta_{1}})\}) \\ &(\operatorname{Diag} &\{\mathbf{a}_{M_{1}}(\omega_{s})\} \otimes \operatorname{Diag} &\{\mathbf{a}_{M_{2}}(\mu_{s})\}) \\ &= &\operatorname{Diag} &\{\mathbf{a}_{M}(-\overline{\varphi_{1}}, -\overline{\theta_{1}})\} \operatorname{Diag} &\{\mathbf{a}_{M}(\omega_{s}, \mu_{s})\}. \end{aligned}$$

Then, combining this equality with (40), A_M is rewritten as

$$\mathbf{A}_{M} = \operatorname{Diag}\{\mathbf{a}_{M}(-\overline{\varphi_{1}}, -\overline{\theta_{1}})\}\operatorname{Diag}\{\mathbf{a}_{M}(\omega_{s}, \mu_{s})\}\mathbf{A}_{\Delta M}$$

$$\stackrel{\triangle}{=} \operatorname{Diag}\{\mathbf{a}_{M}(-\overline{\varphi_{1}}, -\overline{\theta_{1}})\}\mathbf{A}_{s}, \tag{42}$$

where $\mathbf{A}_{\mathrm{s}} = \mathrm{Diag}\{\mathbf{a}_{M}(\omega_{\mathrm{s}}, \mu_{\mathrm{s}})\}\mathbf{A}_{\Delta M}$ can be readily estimated using Algorithm 2. Based on (39) and (42), the common RIS-BS channel matrix \mathbf{H} in (4) is re-expressed as

$$\mathbf{H} = \mathbf{A}_{N} \mathbf{\Lambda} \mathbf{A}_{M}^{\mathrm{H}} = \mathbf{A}_{N} \frac{1}{\overline{\beta}} \mathbf{\Lambda}_{\mathrm{s}} \mathbf{A}_{\mathrm{s}}^{\mathrm{H}} \mathrm{Diag} \{ \mathbf{a}_{M} (\overline{\varphi_{1}}, \overline{\theta_{1}}) \}$$

$$\triangleq \frac{1}{\overline{\beta}} \mathbf{H}_{\mathrm{s}} \mathrm{Diag} \{ \mathbf{a}_{M} (\overline{\varphi_{1}}, \overline{\theta_{1}}) \}, \tag{43}$$

where $\mathbf{H}_{s} = \mathbf{A}_{N} \mathbf{\Lambda}_{s} \mathbf{A}_{s}^{H}$ is the common part of the cascaded channel that can be estimated using Algorithm 1 and Algorithm 2. Then, combining (43) with (38), we have

$$\mathbf{G}_{k} = \mathbf{H} \operatorname{Diag}\{\mathbf{h}_{k}\} = \frac{1}{\overline{\beta}} \mathbf{H}_{s} \operatorname{Diag}\{\mathbf{a}_{M}(\overline{\varphi_{1}}, \overline{\theta_{1}})\} \operatorname{Diag}\{\mathbf{h}_{k}\}$$

$$= \mathbf{H}_{s} \operatorname{Diag}\{\frac{1}{\overline{\beta}} \operatorname{Diag}\{\mathbf{a}_{M}(\overline{\varphi_{1}}, \overline{\theta_{1}})\}\mathbf{h}_{k}\} = \mathbf{H}_{s} \operatorname{Diag}\{\mathbf{h}_{s,k}\},$$
(44)

where $\mathbf{h}_{s,k} = \frac{1}{\beta} \mathrm{Diag}\{\mathbf{a}_M(\overline{\varphi_1}, \overline{\theta_1})\}\mathbf{h}_k$ is the unique part of user k's channel, that needs to be obtained. Next we will show how to estimate the unique part and present the channel estimation strategy for other users, leading to a significant reduction in the pilot overhead.

3) Estimation of Unique Part: Denote the estimate of \mathbf{H}_s as $\widehat{\mathbf{H}}_s = \widehat{\mathbf{A}}_N \widehat{\boldsymbol{\Lambda}}_s \widehat{\mathbf{A}}_s^H$ where $\widehat{\mathbf{A}}_N$, $\widehat{\boldsymbol{\Lambda}}_s$, and $\widehat{\mathbf{A}}_s$ are the estimates of \mathbf{A}_N , $\boldsymbol{\Lambda}_s$, and \mathbf{A}_s , respectively. By replacing \mathbf{H}_s with $\widehat{\mathbf{H}}_s + \Delta \mathbf{H}_s$ where $\Delta \mathbf{H}_s$ represents the error between \mathbf{H}_s and its

estimate, user k's received data Y_k after eliminating the effects of the estimated common AoAs is expressed as

$$\frac{1}{N\sqrt{p}}\widehat{\mathbf{A}}_{N}^{H}\mathbf{Y}_{k} = \frac{1}{N}\widehat{\mathbf{A}}_{N}^{H}\mathbf{H}_{s}\operatorname{Diag}\{\mathbf{h}_{s,k}\}\mathbf{E}_{k} + \frac{1}{N\sqrt{p}}\widehat{\mathbf{A}}_{N}^{H}\mathbf{N}_{k}$$

$$= \widehat{\mathbf{\Lambda}}_{s}\widehat{\mathbf{A}}_{s}^{H}\operatorname{Diag}\{\mathbf{h}_{s,k}\}\mathbf{E}_{k} + \frac{1}{N\sqrt{p}}\widehat{\mathbf{A}}_{N}^{H}\mathbf{N}_{k}$$

$$+ \frac{1}{N}\widehat{\mathbf{A}}_{N}^{H}\Delta\mathbf{H}_{s}\operatorname{Diag}\{\mathbf{h}_{s,k}\}\mathbf{E}_{k}.$$
(45)

For the estimation of $\mathbf{h}_{s,k}$, define $\mathbf{w}_k = \text{vec}(\frac{1}{N\sqrt{p}}\widehat{\mathbf{A}}_N^H\mathbf{Y}_k) \in$ $\mathbb{C}^{L\tau_k\times 1}$. Then, we have

$$\mathbf{w}_{k} = \operatorname{vec}(\widehat{\mathbf{\Lambda}}_{s}\widehat{\mathbf{A}}_{s}^{H}\operatorname{Diag}\{\mathbf{h}_{s,k}\}\mathbf{E}_{k}) + \widetilde{\mathbf{n}}_{k}$$
$$= (\mathbf{E}_{k}^{T} \diamond \widehat{\mathbf{\Lambda}}_{s}\widehat{\mathbf{A}}_{s}^{H})\mathbf{h}_{s,k} + \widetilde{\mathbf{n}}_{k} = \mathbf{W}_{k}\mathbf{h}_{s,k} + \widetilde{\mathbf{n}}_{k}, \quad (46)$$

where $\mathbf{W}_k \triangleq (\mathbf{E}_k^{\mathrm{T}} \diamond \widehat{\mathbf{\Lambda}}_{\mathrm{s}} \widehat{\mathbf{A}}_{\mathrm{s}}^{\mathrm{H}})$ and $\widetilde{\mathbf{n}}_k$ is the corresponding equivalent noise vector given by $\operatorname{vec}(\frac{1}{N\sqrt{p}}\widehat{\mathbf{A}}_N^{\mathrm{H}}\mathbf{N}_k +$ $\frac{1}{N}\widehat{\mathbf{A}}_{N}^{\mathrm{H}}\Delta\mathbf{H}_{\mathrm{s}}\mathrm{Diag}\{\mathbf{h}_{\mathrm{s},k}\}\mathbf{E}_{k})\in\mathbb{C}^{L\tau_{k}\times 1}$. The second equality is obtained via $\mathrm{vec}(\mathbf{A}\mathrm{Diag}\{\mathbf{b}\}\mathbf{C})=(\mathbf{C}^{\mathrm{T}}\diamond\mathbf{A})\mathbf{b}$ [29]. Then, substituting $\mathbf{h}_k = \mathbf{A}_{M,k} \boldsymbol{\beta}_k$ in (5) into $\mathbf{h}_{s,k}$, we have

$$\mathbf{h}_{s,k} = \frac{1}{\overline{\beta}} \operatorname{Diag}\{\mathbf{a}_{M}(\overline{\varphi_{1}}, \overline{\theta_{1}})\} \mathbf{A}_{M,k} \boldsymbol{\beta}_{k}$$

$$= (\mathbf{a}_{M}(\overline{\varphi_{1}}, \overline{\theta_{1}}) \bullet \mathbf{A}_{M,k}) \frac{1}{\overline{\beta}} \boldsymbol{\beta}_{k}, \tag{47}$$

where $\mathbf{a}_{M}(\overline{\varphi_{1}}, \overline{\theta_{1}}) \bullet \mathbf{A}_{M,k} = [\mathbf{a}_{M}(\varphi_{k,1} + \overline{\varphi_{1}}, \theta_{k,1} + \overline{\theta_{1}}), \dots, \mathbf{a}_{M}(\varphi_{k,J_{k}} + \overline{\varphi_{1}}, \theta_{k,J_{k}} + \overline{\theta_{1}})] \in \mathbb{C}^{M \times J_{k}}$. Since both $\varphi_{k,l} + \overline{\varphi_1}$ and $\theta_{k,l} + \overline{\theta_1}$ lie within $[-2\frac{d_{\text{RIS}}}{\lambda_c}, 2\frac{d_{\text{RIS}}}{\lambda_c}]$, we can formulate (46) as a J_k -sparse signal recovery problem

$$\mathbf{w}_{k} = \mathbf{W}_{k} \mathbf{h}_{s,k} + \widetilde{\mathbf{n}}_{k} = \mathbf{W}_{k} (\mathbf{a}_{M}(\overline{\varphi_{1}}, \overline{\theta_{1}}) \bullet \mathbf{A}_{M,k}) \frac{1}{\overline{\beta}} \boldsymbol{\beta}_{k} + \widetilde{\mathbf{n}}_{k}$$
$$= \mathbf{W}_{k} (\mathbf{A}_{1} \otimes \mathbf{A}_{2}) \mathbf{d}_{k} + \widetilde{\mathbf{n}}_{k}. \tag{48}$$

Here $\mathbf{A}_1 \in \mathbb{C}^{M_1 \times D_1}$ and $\mathbf{A}_2 \in \mathbb{C}^{M_2 \times D_2}$ are overcomplete dictionary matrices similar to (28) satisfying $D_1 \geq M_1$ and $D_2 \geq M_2$, and $\mathbf{d}_k \in \mathbb{C}^{D_1 D_2 \times 1}$ is a sparse vector with J_k nonzero entries corresponding to $\{\frac{1}{\beta}\beta_{k,j}\}_{j=1}^{J_k}$. Hence, the angle estimation problem corresponding to (48) can be solved using CS-based techniques. To improve the estimation performance, the alternating optimization (AO) method in [17] can be adopted to optimize the RIS phase shift training matrix \mathbf{E}_k so as to ensure the near column-orthogonality of the equivalent dictionary $W_k(A_1 \otimes A_2)$. In addition, the estimate of the number of scatterers between user-RIS channel for user k, i.e., the sparsity level for the sparse recovery problem associated with (48) J_k , is obtained by the selected CSbased techniques, similarly to the estimation of J_1 discussed before. Note that we obtain the equivalent AoA pair of user k's user-RIS channel, i.e., $(\varphi_{k,j} + \overline{\varphi_1}, \theta_{k,j} + \theta_1)$, by solving angle estimation problem based on (48). The corresponding equivalent AoAs, i.e., $(\varphi_{k,j} + \overline{\varphi_1})$ and $(\theta_{k,j} + \theta_1)$, can be obtained similar to (29). Assume that the p-th element of sparse vector \mathbf{d}_k is nonzero, then the corresponding indices in A_1 and A_2 in (48), denoted by p_1 and p_2 , are derived as

$$p_1 = \left\lceil \frac{p}{D_2} \right\rceil, \quad p_2 = p - D_2(p_1 - 1).$$
 (49)

Finally, we obtain an estimate of the equivalent AoA spatial frequencies for user k's user-RIS channel, i.e., $\{(\varphi_{k,j}+\overline{\varphi_1})\}_{j=1}^{\hat{J}_k}$ and $\{(\theta_{k,j}+\overline{\theta_1})\}_{j=1}^{\hat{J}_k}$. Furthermore, user k's cascaded AoDs, i.e., $(\omega_l-\varphi_{k,j})$ and $(\mu_l-\theta_{k,j})$, for $\forall l \in \{1, \dots, L\}$ and $\forall j \in \{1, \dots, J_k\}$, can be also obtained as follows:

$$\omega_{l} - \varphi_{k,j} = \omega_{r} + \overline{\varphi_{1}} - (\overline{\varphi_{1}} + \varphi_{k,j}) + \omega_{l} - \omega_{r}$$

$$= \omega_{s} - (\overline{\varphi_{1}} + \varphi_{k,j}) + \Delta\omega_{l}, \qquad (50a)$$

$$\mu_{l} - \theta_{k,j} = \mu_{r} + \overline{\theta_{1}} - (\overline{\theta_{1}} + \theta_{k,j}) + \mu_{l} - \mu_{r}$$

$$= \mu_{s} - (\overline{\theta_{1}} + \theta_{k,j}) + \Delta\mu_{l}. \qquad (50b)$$

Based on (31), (41) and (48), the parameters $\Delta\omega_l$, $\Delta\mu_l$, $\omega_{\rm s}, \ \mu_{\rm s}, \ (\overline{\varphi_1} + \varphi_{k,j}) \ \ {\rm and} \ \ (\overline{\theta_1} + \theta_{k,j}) \ \ {\rm for} \ \ \forall l \in \{1,2,\ldots,L\}$ and $\forall j \in \{1, 2, \dots, J_k\}$ can be readily estimated. Finally, the completed CS-based estimation of G_k for $2 \le k \le K$ is summarized in Algorithm 3. As shown in Algorithm 3, the obtained common part of cascaded channel H_s allows us to estimate the unique part $\mathbf{h}_{s,k}$ with reduced pilot overhead.

Algorithm 3 Estimation of Full CSI for Other Users

Input: \mathbf{Y}_k , \mathbf{A}_N .

- 1: Obtain the estimate $\hat{\Lambda}_s$ based on (39);
- 2: Obtain the estimate A_s based on (42);
- 3: Obtain the estimate of the common part, i.e., $H_s =$ $\hat{\mathbf{A}}_N \hat{\mathbf{\Lambda}}_{\mathrm{s}} \hat{\mathbf{A}}_{\mathrm{s}}^{\mathrm{H}};$
- 4: **for** $2 \le k \le K$ **do**
- Calculate $\mathbf{w}_k = \mathrm{vec}(\frac{1}{N\sqrt{p}}\widehat{\mathbf{A}}_N^H\mathbf{Y}_k);$ Calculate equivalent dictionary $\mathbf{W}_k(\mathbf{A}_1 \otimes \mathbf{A}_2)$ according to (46);
- Estimate unique part $h_{s,k}$ by solving sparse recovery problem associated with (48);
- Obtain the estimate of cascaded channel, i.e., $\mathbf{G}_k = \mathbf{H}_s \mathrm{Diag}\{\mathbf{h}_{s,k}\};$

9: end for

Output: $\hat{\mathbf{G}}_k$, $2 \leq k \leq K$.

C. Pilot Overhead and Computational Complexity Analysis

In this subsection, we first analyze the pilot overhead required for the full CSI estimation. Then, the corresponding computational complexity is evaluated. For simplicity, $J_1 = J_2 = \cdots = J_K = J$ is assumed.

1) Pilot Overhead Analysis: Clearly, the number of pilot symbols directly affects the sparse recovery performance for equations (28) and (48). According to [30], to find a *l*-sparse complex signal (vector) with dimension n, the number of measurements m is required to be on the order of $\mathcal{O}(l \log(n))$, which is proportional to the sparsity level l.

Based on this fact, we first analyze the number of pilots required for the typical user, i.e., user 1. For the sparse recovery problem associated with (28) in Stage I, the dimension of the equivalent sensing matrix $\mathbf{F}_1 \triangleq \mathbf{E}_1^{\mathrm{H}}(\mathbf{A}_1 \otimes \mathbf{A}_2)$ is $\tau_1 \times D_1 D_2$ where $D_1 \geq M_1$ and $D_2 \geq M_2$, and the corresponding sparsity level is J_1 , thus the pilot overhead required for user 1 should satisfy $\tau_1 \geq \mathcal{O}(J_1 \log(D_1 D_2)) \geq$ $\mathcal{O}(J_1 \log(M_1 M_2)) = \mathcal{O}(J_1 \log(M)).$

For the sparse recovery problem associated with (48) in Stage II, the dimension of the equivalent sensing matrix $\mathbf{F}_k \triangleq \mathbf{W}_k(\mathbf{A}_1 \otimes \mathbf{A}_2)$ is $L\tau_k \times D_1D_2$ where $D_1 \geq M_1$ and $D_2 \geq M_2$, and the corresponding sparsity level is J_k , thus user k needs $\tau_k \geq \mathcal{O}(J_k\log(D_1D_2)/L) \geq \mathcal{O}(J_k\log(M_1M_2)/L) = \mathcal{O}(J_k\log(M)/L)$ pilot symbols. Therefore, the overall required pilot overhead in the first coherence block is $\mathcal{O}(J\log(M) + (K-1)J\log(M)/L)$.

2) Computational Complexity Analysis: For the estimation of the typical user in Stage I shown in Algorithm 2, the computational complexity mainly stems from Algorithm 1 in Step 1, the CS-based method for the estimation of $\mathbf{h}_{RIS,r}$ in Step 3 and the correlation based scheme in Step 5. Specifically, the dominant complexity for Algorithm 1 are calculating the matrix multiplication in its Step 1 with computational complexity of $\mathcal{O}(N^2\tau_1)$ and implementing the angle rotation in its Step 7 with computational complexity of $\mathcal{O}(N\tau_1L(g_1+g_2))$. We take OMP as the recovery algorithm, whose corresponding dominant complexity is $\mathcal{O}(mnl)$ [17], where m is the length of the measurements, and n is the length of the sparse signal with sparsity level l. Hence, the complexity for estimating $\mathbf{h}_{RIS,r}$ is $\mathcal{O}(\tau_1 D_1 D_2 J_1)$. Additionally, the computational complexity of the correlation based scheme is given by $\mathcal{O}(M\tau_1(L 1)d_1d_2$), where d_1 and d_2 represent the search grids for $\Delta\omega_l$ and $\Delta\mu_l$ within $[-2\frac{d_{\rm RIS}}{\lambda_c}, 2\frac{d_{\rm RIS}}{\lambda_c}]$, respectively. The overall computational complexity in Stage I is $\mathcal{O}(\tau_1 D_1 D_2 J + N^2 \tau_1 +$ $N\tau_1L(g_1+g_2)+M\tau_1(L-1)d_1d_2$).

Then, we analyze the computational complexity for the estimation of other users in Stage II shown in Algorithm 3, which mainly stems from the CS-based method for estimation of $\mathbf{h}_{s,k}$ in Step 7. Similarly, we choose OMP to solve the sparse recovery problem associated with (48), and thus the corresponding computational complexity is $\mathcal{O}(\tau_k L D_1 D_2 J_k)$. Consider (K-1) users in total, the overall computational complexity in Stage II during the first coherence block is $\mathcal{O}((K-1)\tau_k L D_1 D_2 J)$.

IV. CHANNEL ESTIMATION IN REMAINING COHERENCE BLOCKS

After the first coherence block, we adopt the LS estimator to re-estimate the cascaded gains since the angles remain unchanged during the remaining coherence blocks. Later we will see the required pilot overhead can be reduced further in this stage.

Without loss of generality, we consider an arbitrary k from \mathcal{K} and show how to re-estimate user k's channel gains. Similar to (25), we first take user k's equivalent measurement matrix $\overline{\mathbf{Y}}_k$, i.e., $\overline{\mathbf{Y}}_k = (\frac{1}{N\sqrt{p}}\widehat{\mathbf{A}}_N^{\mathrm{H}}\mathbf{Y}_k)^{\mathrm{H}} \in \mathbb{C}^{\tau_k \times L}$, where $\widehat{\mathbf{A}}_N$ has been acquired in Stage I. Then, following the same derivations as for (27), the r-th column of $\overline{\mathbf{Y}}_k$, denoted as $\overline{\mathbf{y}}_{k,r}$, is given by

$$\overline{\mathbf{y}}_{k,r} = \mathbf{E}_{k}^{\mathrm{H}} (\mathbf{A}_{M,k}^{*} \bullet \mathbf{a}_{M}(\omega_{r}, \mu_{r})) \alpha_{r}^{*} \boldsymbol{\beta}_{k}^{*} + \overline{\mathbf{n}}_{k,r}$$

$$\triangleq \mathbf{E}_{k}^{\mathrm{H}} \mathbf{V}_{k,r} \alpha_{r}^{*} \boldsymbol{\beta}_{k}^{*} + \overline{\mathbf{n}}_{k,r}. \tag{51}$$

Here, $\mathbf{V}_{k,r} \triangleq \mathbf{A}_{M,k}^* \bullet \mathbf{a}_M(\omega_r, \mu_r) = [\mathbf{a}_M(\omega_r - \varphi_{k,1}, \mu_r - \theta_{k,1}), \dots, \mathbf{a}_M(\omega_r - \varphi_{k,J_k}, \mu_r - \theta_{k,J_k})] \in \mathbb{C}^{M \times J_k}$ and $\overline{\mathbf{n}}_{k,r}$ is the r-th column of $[\frac{1}{N\sqrt{p}}\widehat{\mathbf{A}}_N^{\mathrm{H}}(\mathbf{N}_k + \sqrt{p}\Delta\mathbf{A}_N\mathbf{\Lambda}\mathbf{A}_M^{\mathrm{H}}\mathrm{Diag}\{\mathbf{h}_k\}\mathbf{E}_k)]^{\mathrm{H}}$. We have already obtained

an estimate of $\mathbf{V}_{k,r}$, denoted by $\widehat{\mathbf{V}}_{k,r}$, in the first coherence block. Specifically, for the typical user, i.e., user 1, $\{(\omega_r-\varphi_{1,j},\mu_r-\theta_{1,j})\}_{j=1}^{J_1}$ are estimated from (27) and (37) in Stage I, while for other users, $\{(\omega_r-\varphi_{k,j},\mu_r-\theta_{k,j})\}_{j=1}^{J_k}$ are estimated from (50) in Stage II.

The updated cascaded channel gain $\beta_k^*\alpha_r^*$ in (51) can be found using the LS estimator

$$\widehat{\boldsymbol{\beta}_{k}^{*}\alpha_{r}^{*}} = (\widehat{\mathbf{V}}_{k,r}^{\mathrm{H}} \mathbf{E}_{k} \mathbf{E}_{k}^{\mathrm{H}} \widehat{\mathbf{V}}_{k,r})^{-1} \widehat{\mathbf{V}}_{k,r}^{\mathrm{H}} \mathbf{E}_{k} \overline{\mathbf{y}}_{k,r}.$$
(52)

Then, following the same operation shown in (36), and substituting (52) into (51), the estimate of user k's cascaded channel during the remaining coherence blocks is given by

$$\widehat{\mathbf{G}}_{k} = \widehat{\mathbf{A}}_{N} \widehat{\mathbf{H}}_{\mathrm{RIS},k}^{\mathrm{H}} = \widehat{\mathbf{A}}_{N} [\widehat{\mathbf{h}}_{\mathrm{RIS}k,1}, \dots, \widehat{\mathbf{h}}_{\mathrm{RIS}k,L}]^{\mathrm{H}}$$

$$= \widehat{\mathbf{A}}_{N} [\widehat{\mathbf{V}}_{k,1} \widehat{\boldsymbol{\beta}_{k}^{*} \alpha_{1}^{*}}, \dots, \widehat{\mathbf{V}}_{k,L} \widehat{\boldsymbol{\beta}_{k}^{*} \alpha_{L}^{*}}]^{\mathrm{H}}, \tag{53}$$

where $\mathbf{h}_{RISk,r}$ represents the r-th column of $\mathbf{H}_{RIS,k}$.

For the pilot overhead analysis, we assume $J_1 = J_2 = \cdots = J_K = J$ as before. For the LS problem in (51), $\tau_k \geq J_k$ should hold for user k. Thus, the minimum number of pilot symbols can be chosen as $\tau_k = J_k$, which is less than that required in Stage II. Given K total users, the overall minimum pilot overhead is JK. On the other hand, the dominant complexity of LS problem in (51) is $\mathcal{O}(\tau_k J^2)$. Since obtaining the entire cascaded channel, i.e., G_k , needs to solve the LS problem L times, the total computational complexity for user k is $\mathcal{O}(\tau_k J^2 L)$. Thus the overall computational complexity in each remaining coherence block is $\mathcal{O}(\tau_k J^2 LK)$.

V. EXTENSION TO MULTI-ANTENNA USER CASE

In this section, we extend the full CSI estimation method in the first coherence block to the multi-antenna user case. First, the system model and corresponding two-phase channel estimation strategy are described. Then, we adopt an OMP-based method to estimate the AoDs at the users in Phase I. The remaining parameters including the common AoAs at the BS, the cascaded AoDs at the RIS, and the cascaded gains are estimated in Phase II, similarly to the methods developed for the single-antenna user case in Section III. Lastly, the required pilot overhead and computation complexity for the proposed method are analyzed.

A. Multi-Antenna Users Model and Channel Estimation Strategy

1) System Model: We assume that K users are present with an $Q_k = Q_{k1} \times Q_{k2}$ UPA for user k, while the other settings are the same as in the single-antenna user case. Then, \mathbf{h}_k in (3) and (5) can be modified as

$$\mathbf{H}_{k} = \sum_{j=1}^{J_{k}} \beta_{k,j} \mathbf{a}_{M}(\varphi_{k,j}, \theta_{k,j}) \mathbf{a}_{Q_{k}}^{\mathrm{H}}(\eta_{k,j}, \chi_{k,j})$$
$$= \mathbf{A}_{M,k} \mathbf{B}_{k} \mathbf{A}_{Q,k}^{\mathrm{H}} \in \mathbb{C}^{M \times Q_{k}}, \quad \forall k \in \mathcal{K},$$
(54)

⁷The re-estimation of channel gains in the remaining coherence blocks can be extended to the multi-antenna-users case in a straightforward way, and thus will not be explicitly considered.

where $(\eta_{k,j},\chi_{k,j})$ represents the AoD of the j-th path in the user k-RIS channel, and $\mathbf{A}_{Q,k} = [\mathbf{a}_{Q_k}(\eta_{k,1},\chi_{k,1}),\ldots,\mathbf{a}_{Q_k}(\eta_{k,J_k},\chi_{k,J_k})] \in \mathbb{C}^{Q_k \times J_k}$ and $\mathbf{B}_k = \mathrm{Diag}\{\beta_{k,1},\ldots,\beta_{k,J_k}\} \in \mathbb{C}^{J_k \times J_k}$ are the AoD steering matrix and complex gain matrix of user k, respectively. Other parameters are as defined in Section II. With \mathbf{H}_k , the transmission model in (6) becomes

$$\mathbf{y}_k(t) = \mathbf{H}\mathrm{Diag}\{\mathbf{e}_t\}\mathbf{H}_k\sqrt{p}\mathbf{s}_k(t) + \mathbf{n}_k(t),$$
 (55)

where $\mathbf{s}_k(t) \in \mathbb{C}^{Q_k \times 1}$ is the pilot vector for user k in time slot t. Vectorizing (55), we have

$$\mathbf{y}_{k}(t) = \sqrt{p}(\mathbf{s}_{k}^{\mathrm{T}}(t) \otimes \mathbf{I}_{N}) \operatorname{vec}(\mathbf{H}\operatorname{Diag}\{\mathbf{e}_{t}\}\mathbf{H}_{k}) + \mathbf{n}_{k}(t)$$

$$\triangleq \sqrt{p}(\mathbf{s}_{k}^{\mathrm{T}}(t) \otimes \mathbf{I}_{N}) \mathbf{G}_{k} \mathbf{e}_{t} + \mathbf{n}_{k}(t), \tag{56}$$

where \mathbf{I}_N represents the $N \times N$ identity matrix, and $\mathbf{G}_k = \mathbf{H}_k^{\mathrm{T}} \diamond \mathbf{H}$ is the cascaded user-RIS-BS channel of user k that is to be estimated. The above equality is also obtained via $\operatorname{vec}(\mathbf{A}\operatorname{Diag}\{\mathbf{b}\}\mathbf{C}) = (\mathbf{C}^{\mathrm{T}} \diamond \mathbf{A})\mathbf{b}$. Combining (54) with (4), \mathbf{G}_k can be rewritten as

$$\mathbf{G}_{k} = (\mathbf{A}_{M,k} \mathbf{B}_{k} \mathbf{A}_{Q,k}^{\mathrm{H}})^{\mathrm{T}} \diamond (\mathbf{A}_{N} \boldsymbol{\Lambda} \mathbf{A}_{M}^{\mathrm{H}})$$

$$= (\mathbf{A}_{Q,k}^{*} \otimes \mathbf{A}_{N}) (\mathbf{B}_{k}^{\mathrm{T}} \otimes \boldsymbol{\Lambda}) (\mathbf{A}_{M,k}^{\mathrm{T}} \diamond \mathbf{A}_{M}^{\mathrm{H}})$$

$$= (\mathbf{A}_{Q,k}^{*} \otimes \mathbf{A}_{N}) (\mathbf{B}_{k} \otimes \boldsymbol{\Lambda}) (\mathbf{A}_{M,k} \bullet \mathbf{A}_{M}^{*})^{\mathrm{T}}, \quad (57)$$

where the above equalities are obtained using $(\mathbf{A} \otimes \mathbf{B})(\mathbf{C} \otimes \mathbf{D}) = (\mathbf{AC}) \diamond (\mathbf{BD})$ and $\mathbf{A}^{\mathrm{T}} \diamond \mathbf{B}^{\mathrm{T}} = (\mathbf{A} \bullet \mathbf{B})^{\mathrm{T}}$ [28], [29]. The third term $(\mathbf{A}_{M,k} \bullet \mathbf{A}_{M}^{*})$ accounts for the cascaded AoDs at the RIS, similar to the single-antenna user case.

2) Channel Estimation Strategy: For the full-CSI estimation of any user k, a two-phase estimation strategy is adopted, where the AoDs at the users, i.e., $\mathbf{A}_{Q,k}$, is estimated in Phase I, after which the remaining parameters in (57) are estimated in Phase II. Specifically, in this strategy, Υ_k blocks of time slots are used for the channel estimation of user k, and the i-th block has $V_k^{(i)}$ time slots. The RIS phase shift vector remains invariant for each time slot within a given block, and is denoted by $\mathbf{e}^{(i)}$ for $\forall i \in \{1,2,\ldots,\Upsilon_k\}$. Later we will see that Phase I only occurs in the first block, and $V_k^{(i)}$ can be different for different users or/and different blocks, while Phase II consists of the whole blocks.

B. Estimation in Phase I: Angle Estimation at Users

In this subsection, we describe the estimation of the AoDs at the users.

During the first block, user k transmits the pilot sequence $\mathbf{S}_k^{(1)} = \left[\mathbf{s}_1^{(1)}, \dots, \mathbf{s}_{V_k^{(1)}}^{(1)}\right] \in \mathbb{C}^{Q_k \times V_k^{(1)}}$, and the received signal matrix $\mathbf{Y}_k^{(1)} = \left[\mathbf{y}_k^{(1)}(1), \dots, \mathbf{y}_k^{(1)}(V_k^{(1)})\right] \in \mathbb{C}^{N \times V_k^{(1)}}$ at the BS is given by

$$\mathbf{Y}_{k}^{(1)} = \sqrt{p}\mathbf{H}\operatorname{Diag}\{\mathbf{e}^{(1)}\}\mathbf{H}_{k}\mathbf{S}_{k}^{(1)} + \mathbf{N}_{k}^{(1)}$$
$$= \sqrt{p}\mathbf{A}_{N}\mathbf{\Lambda}\mathbf{A}_{M}^{H}\operatorname{Diag}\{\mathbf{e}^{(1)}\}\mathbf{A}_{M,k}\mathbf{B}_{k}\mathbf{A}_{Q,k}^{H}\mathbf{S}_{k}^{(1)} + \mathbf{N}_{k}^{(1)}.$$
(58)

 $\mathbf{A}_{Q,k}$ can be directly obtained from (58).

Specifically, for the estimation of $A_{Q,k}$, an OMP-based method can be adopted, which takes the transpose of (58)

and formulates it as a simultaneously sparse approximation problem [18], [31]

$$(\mathbf{Y}_{k}^{(1)})^{\mathrm{H}} = (\mathbf{S}_{k}^{(1)})^{\mathrm{H}} \mathbf{A}_{Q,k} \mathbf{\Gamma}_{k} + (\mathbf{N}_{k}^{(1)})^{\mathrm{H}} \in \mathbb{C}^{V_{k}^{(1)} \times N},$$
 (59)

where Γ_k represents the remaining terms according to (58). Similar to equations (28) and (48), by using the VAD representation, (59) can be approximated as

$$(\mathbf{Y}_{k}^{(1)})^{\mathrm{H}} = (\mathbf{S}_{k}^{(1)})^{\mathrm{H}} (\mathbf{A}_{Q,1} \otimes \mathbf{A}_{Q,2}) \widetilde{\mathbf{\Gamma}}_{k} + (\mathbf{N}_{k}^{(1)})^{\mathrm{H}},$$
 (60)

where $\mathbf{A}_{Q,1} \in \mathbb{C}^{Q_{k1} \times D_1}$ and $\mathbf{A}_{Q,2} \in \mathbb{C}^{Q_{k1} \times D_2}$ are overcomplete dictionary matrices $(D_1 \geq Q_{k1}, D_2 \geq Q_{k1})$ similar to (28), and contain values for $\mathbf{a}_{Q_{k1}}(\eta_{k,j})$ and $\mathbf{a}_{Q_{k2}}(\chi_{k,j})$. $\widetilde{\Gamma}_k \in \mathbb{C}^{D_1 D_2 \times N}$ is a row-sparse matrix with J_k non-zero rows. Similar to the single-antenna user case in Section III, the sparsity level for the sparse recovery problem associated with (60) J_k , is obtained by OMP. Therefore, the AoDs at user k, i.e., $\{\eta_{k,j}\}_{j=1}^{J_k}$ and $\{\chi_{k,j}\}_{j=1}^{J_k}$ can be obtained similar to (29). Assume the q-th row of the sparse matrix $\widetilde{\Gamma}_k$ is nonzero, then the corresponding indices in $\mathbf{A}_{Q,1}$ and $\mathbf{A}_{Q,2}$ in (60), denoted by q_1 and q_2 , are derived as

$$q_1 = \left\lceil \frac{q}{D_2} \right\rceil, \quad q_2 = q - D_2(q_1 - 1).$$
 (61)

C. Estimation in Phase II: Estimation of Remaining Parameters

In this subsection, we estimate the remaining parameters in (57) by converting the estimation problems into several equivalent problems as in the single-antenna user case, which can be solved using the methods in Section III.

First, denote the typical user as user 1 and stack the total $(\sum_{i=1}^{\Upsilon_1} V_1^{(i)})$ slots, the received signal matrix is obtained as $\mathbf{Y}_1 = \left[\mathbf{Y}_1^{(1)}, \dots, \mathbf{Y}_1^{(\Upsilon_1)}\right] \in \mathbb{C}^{N \times (\sum_{i=1}^{\Upsilon_1} V_1^{(i)})}$. Then, the common AoAs in (57), i.e., \mathbf{A}_N , can be readily estimated via DFT-based method by calculating $\widetilde{\mathbf{U}}_N^{\mathrm{H}} \mathbf{Y}_1$ since Lemma 2 holds.

With $\widehat{\mathbf{A}}_{Q,k}$ obtained in Phase I and $\widehat{\mathbf{A}}_N$ obtained in Phase II, considering the i-th time block and replacing \mathbf{A}_N and $\mathbf{A}_{Q,k}$ with $\widehat{\mathbf{A}}_N + \Delta \mathbf{A}_N$ and $\widehat{\mathbf{A}}_{Q,k} + \Delta \mathbf{A}_{Q,k}$, respectively, $\mathbf{Y}_k^{(i)} \in \mathbb{C}^{N \times V_k^{(i)}}$ can be processed as

$$\check{\mathbf{Y}}_{k}^{(i)} \triangleq \frac{1}{N\sqrt{p}} \widehat{\mathbf{A}}_{N}^{H} \mathbf{Y}_{k}^{(i)} (\widehat{\mathbf{A}}_{Q,k}^{H} \mathbf{S}_{k}^{(i)})^{\dagger}
= \frac{1}{N\sqrt{p}} \widehat{\mathbf{A}}_{N}^{H} \{ (\widehat{\mathbf{A}}_{N} + \Delta \mathbf{A}_{N}) \mathbf{\Lambda} \mathbf{A}_{M}^{H} \text{Diag} \{ \mathbf{e}^{(i)} \}
\mathbf{A}_{M,k} \mathbf{B}_{k} (\widehat{\mathbf{A}}_{Q,k} + \Delta \mathbf{A}_{Q,k})^{H} \mathbf{S}_{k}^{(i)} + \mathbf{N}_{k}^{(i)} \} (\widehat{\mathbf{A}}_{Q,k}^{H} \mathbf{S}_{k}^{(i)})^{\dagger}
= \mathbf{\Lambda} \mathbf{A}_{M}^{H} \text{Diag} \{ \mathbf{e}^{(i)} \} \mathbf{A}_{M,k} \mathbf{B}_{k} + \check{\mathbf{N}}_{k}^{(i)} \in \mathbb{C}^{L \times J_{k}}, \quad (62)$$

where $\Delta \mathbf{A}_N$ and $\Delta \mathbf{A}_{Q,k}$ stand for the estimation errors of \mathbf{A}_N and $\mathbf{A}_{Q,k}$, respectively. $\check{\mathbf{N}}_k^{(i)}$ represents the remaining terms of the second equality. As discussed in Remark 1, all users are allowed to estimate the common \mathbf{A}_N jointly so as to acquire the MU diversity gains to alleviate the error propagation effects caused by $\Delta \mathbf{A}_N$. Accordingly, the input of Algorithm 1 is given by $\mathbf{Y} = [\mathbf{Y}_1, \mathbf{Y}_2, \dots, \mathbf{Y}_K] \in \mathbb{C}^{N \times (\sum_{k=1}^K \sum_{i=1}^{r_k} V_k^{(i)})}$.

In the following, we decompose the estimation of a multi-antenna user, i.e., user k, with a channel composed of J_k scatterers, into the estimation of J_k channels with a single path for a virtual single-antenna user, i.e., user (k,j) for $j \in \{1,\ldots,J_k\}$. The j-th column of $\check{\mathbf{Y}}_k^{(i)}$ is given by

$$[\check{\mathbf{Y}}_{k}^{(i)}]_{(:,j)} = \mathbf{\Lambda} \mathbf{A}_{M}^{\mathrm{H}} \mathrm{Diag} \{ \mathbf{e}^{(i)} \} [\mathbf{A}_{M,k}]_{(:,j)} \beta_{k,j} + [\check{\mathbf{N}}_{k}^{(i)}]_{(:,j)}$$

$$= \mathbf{\Lambda} \mathbf{A}_{M}^{\mathrm{H}} \mathrm{Diag} \{ [\mathbf{A}_{M,k}]_{(:,j)} \beta_{k,j} \} \mathbf{e}^{(i)} + [\check{\mathbf{N}}_{k}^{(i)}]_{(:,j)}.$$
(63)

Stacking Υ_k blocks of (63), we have

$$\begin{split}
&\left[\left[\check{\mathbf{Y}}_{k}^{(1)}\right]_{(:,j)}, \dots, \left[\check{\mathbf{Y}}_{k}^{(\Upsilon_{k})}\right]_{(:,j)}\right] \\
&= \mathbf{\Lambda} \mathbf{A}_{M}^{H} \operatorname{Diag}\left\{\left[\mathbf{A}_{M,k}\right]_{(:,j)} \beta_{k,j}\right\} \widetilde{\mathbf{E}}_{k} \\
&+ \left[\left[\check{\mathbf{N}}_{k}^{(1)}\right]_{(:,j)}, \dots, \left[\check{\mathbf{N}}_{k}^{(\Upsilon_{k})}\right]_{(:,j)}\right] \\
&= \mathbf{\Lambda} \mathbf{A}_{M}^{H} \operatorname{Diag}\left\{\widetilde{\mathbf{h}}_{\{k,j\}}\right\} \widetilde{\mathbf{E}}_{k} \\
&+ \left[\left[\check{\mathbf{N}}_{k}^{(1)}\right]_{(:,j)}, \dots, \left[\check{\mathbf{N}}_{k}^{(\Upsilon_{k})}\right]_{(:,j)}\right],
\end{split} (64)$$

where $\widetilde{\mathbf{E}}_k = \left[\mathbf{e}^{(1)}, \dots, \mathbf{e}^{(\Upsilon_k)}\right] \in \mathbb{C}^{M \times \Upsilon_k}$. The term $\widetilde{\mathbf{h}}_{\{k,j\}} \triangleq \left[\mathbf{A}_{M,k}\right]_{(:,j)} \beta_{k,j} \in \mathbb{C}^{M \times 1}$ is treated as the channel between the RIS and the virtual single-antenna user (k,j), which only contains one scatterer.

1) Estimation for Typical User: This part is the extension of Section III-A for the typical user, i.e., user 1. Denote the transpose of (64) for user 1 as $\widetilde{\mathbf{Y}}_{\{1,j\}} \in \mathbb{C}^{\Upsilon_1 \times L}$, which is given by

$$\widetilde{\mathbf{Y}}_{\{1,j\}} = \widetilde{\mathbf{E}}_{1}^{\mathrm{H}} \mathrm{Diag}\{\widetilde{\mathbf{h}}_{\{1,j\}}^{*}\} \mathbf{A}_{M} \mathbf{\Lambda}^{*} + \widetilde{\mathbf{N}}_{\{1,j\}}. \tag{65}$$

We note that the channel estimation problem for (65) has a form similar to that for (25), and can be solved following the steps developed in Section III-A. Thus the virtual single-antenna cascaded AoDs for user (1,j), i.e., $\{(\omega_l-\varphi_{1,j})\}_{l=1}^L$ and $\{(\mu_l-\theta_{1,j})\}_{l=1}^L$, and the cascaded gains $\{\alpha_l\beta_{1,j}\}_{l=1}^L$ can be estimated.

It is unnecessary for us to repeat the steps shown in Section III-A J_1 times to solve the angle estimation problem connected with (65). That is because we have obtained the rotation factors $(\Delta\omega_l, \Delta\mu_l)$ and gain scaling factor γ_l defined in (31) after the estimation procedure for the first virtual single-antenna user, user (1,1). This allows us to solve the sparse recovery problem corresponding to (27) without performing additional operations for the channel estimation of the other virtual single-antenna users (1, j) for $j \neq 1.8$ In particular, for user (1, j), the quantities $(\omega_r - \varphi_{1,j})$, $(\mu_r - \theta_{1,j})$ and $\alpha_r^* \beta_{1,j}^*$ can be obtained via the solution to (27). Then, $\{(\omega_l - \varphi_{1,j})\}_{l \neq r}, \{(\mu_r - \theta_{1,j})\}_{l \neq r} \text{ and } \{\alpha_l^* \beta_{1,j}^*\}_{l \neq r} \text{ can be}$ directly obtained with the known $(\Delta\omega_l, \Delta\mu_l)$ and γ_l obtained in the estimation for user (1,1). Based on this, the estimates of user 1's cascaded gains and cascaded AoDs at the RIS, i.e., $\alpha_l \beta_{1,j}$, $(\omega_l - \varphi_{1,j})$ and $(\mu_l - \theta_{1,j})$, for $\forall l \in \{1, \ldots, L\}$ and $\forall j \in \{1, \dots, J_1\}$, are obtained, which allows us to determine \mathbf{G}_1 in (57).

2) Estimation for Other Users: Following the idea of the virtual single-antenna user, we convert the channel estimation for the other multi-antenna users into the estimation of $\sum_{k=2}^{K} J_k$ single scatterer channels for the other single-antenna users. The idea of constructing the common part as in Section III-B still applies, using the common RIS-BS channel to reduce the pilot overhead.

Specifically, after eliminating the effects of the common AoAs at the BS, and the unique AoDs at the users estimated in Phase I, and following (45), $[\check{\mathbf{Y}}_k^{(i)}]_{(:,j)}$ in (63) can be reformulated as

$$\begin{split} [\check{\mathbf{Y}}_{k}^{(i)}]_{(:,j)} &= \mathbf{\Lambda} \mathbf{A}_{M}^{\mathrm{H}} \mathrm{Diag}\{\widetilde{\mathbf{h}}_{\{k,j\}}\} \mathbf{e}^{(i)} + [\check{\mathbf{N}}_{k}^{(i)}]_{(:,j)} \\ &= \widetilde{\mathbf{\Lambda}}_{\mathrm{s}} \widetilde{\mathbf{A}}_{\mathrm{s}}^{\mathrm{H}} \mathrm{Diag}\{\widetilde{\mathbf{h}}_{\mathrm{s},\{k,j\}}\} \mathbf{e}^{(i)} + [\check{\mathbf{N}}_{k}^{(i)}]_{(:,j)}, \quad (66) \end{split}$$

where $\widetilde{\mathbf{A}}_{\mathrm{s}} = \alpha_r \beta_{1,1} \mathrm{Diag}\{\gamma_1^*, \gamma_2^*, \dots, \gamma_L^*\}$ and $\widetilde{\mathbf{A}}_{\mathrm{s}} = \mathrm{Diag}\{\mathbf{a}_M(\omega_r - \varphi_{1,1}, \mu_r - \theta_{1,1})\}\mathbf{A}_{\Delta M}$ can be constructed using the estimated parameters of the virtual single-antenna user (1,1). The matrix $\mathbf{A}_{\Delta M}$ can be determined by (40). Accordingly, $\widetilde{\mathbf{h}}_{\mathrm{s},\{k,j\}} = \frac{1}{\beta_{1,1}}\mathrm{Diag}\{\mathbf{a}_M(-\varphi_{1,1},-\theta_{1,1})\}\widetilde{\mathbf{h}}_{\{k,j\}}$ is the unique part of the cascaded channel for virtual single-antenna user (k,j) that is to be estimated. Stacking Υ_k time blocks of (66) and vectorizing, we have

$$\widetilde{\mathbf{w}}_{\{k,j\}} \triangleq \operatorname{vec}(\left[[\check{\mathbf{Y}}_{k}^{(1)}]_{(:,j)}, \dots, [\check{\mathbf{Y}}_{k}^{(\Upsilon_{k})}]_{(:,j)} \right])
= (\widetilde{\mathbf{E}}_{k}^{\mathrm{T}} \diamond \widetilde{\mathbf{\Lambda}}_{s} \widetilde{\mathbf{A}}_{s}^{\mathrm{H}}) \widetilde{\mathbf{h}}_{s,\{k,j\}} + \widetilde{\mathbf{n}}_{\{k,j\}} \in \mathbb{C}^{L\Upsilon_{k} \times 1}, \quad (67)$$

where $\widetilde{\mathbf{n}}_{\{k,j\}}$ is the corresponding equivalent noise for virtual user (k,j). The last equality is obtained via $\operatorname{vec}(\widetilde{\mathbf{\Lambda}}_{\mathbf{s}}\widetilde{\mathbf{A}}_{\mathbf{s}}^{\mathrm{H}}\operatorname{Diag}\{\widetilde{\mathbf{h}}_{\mathbf{s},\{k,j\}}\}\widetilde{\mathbf{E}}_{k}) = (\widetilde{\mathbf{E}}_{k}^{\mathrm{T}} \diamond \widetilde{\mathbf{\Lambda}}_{\mathbf{s}}\widetilde{\mathbf{A}}_{\mathbf{s}}^{\mathrm{H}})\widetilde{\mathbf{h}}_{\mathbf{s},\{k,j\}}$. Since the form of (67) is similar to (46), $\widetilde{\mathbf{h}}_{\mathbf{s},\{k,j\}}$ can be estimated similarly to what was done for (48).

With the estimates of the multi-antenna user k's cascaded gains and cascaded AoDs, i.e., $\alpha_l \beta_{k,j}$, $(\omega_l - \varphi_{k,j})$ and $(\mu_l - \theta_{k,j})$, for $\forall l \in \{1,\ldots,L\}$, $\forall j \in \{1,\ldots,J_k\}$, obtained by solving the problem connected with (67) J_k times, \mathbf{G}_k in (57) can be determined for $\forall k \in \{2,3\ldots,K\}$.

D. Pilot Overhead Analysis

In this subsection, we analyze the pilot overhead of the full CSI estimation algorithm for the multi-antenna user case, assuming $J_1=J_2=\cdots=J_K=J$ and $Q_1=Q_2=\cdots=Q_k=Q$.

Similar to the analysis in Section III-C.1, for user 1, the number of time slots in Phase I should satisfy $V_1^{(1)} \geqslant \mathcal{O}(J_1\log(D_1D_2)) \geqslant \mathcal{O}(J_1\log(Q_{11}Q_{12})) = \mathcal{O}(J_1\log(Q_1))$ so as to ensure the J_1 -sparse recovery problem associated with (60). In Phase II, the number of time slots within each block $V_1^{(i)}$, should satisfy $V_1^{(i)} \geqslant J_1$, otherwise the right inverse $(\mathbf{A}_{Q,1}^{\mathrm{H}}\mathbf{S}_1^{(i)})^{\dagger}$ does not exist. On the other hand, the number of blocks, Υ_1 , is determined by sparse recovery applied to (65). The angle estimation associated with (65) can be implemented

⁸The virtual single-antenna users (1,j) for $j \neq 1$ can be treated as other users and the corresponding parameters can be estimated by the method shown later. However, the pilot overhead for virtual users (1,j) for any j should be the same, depending on the the number of time blocks Υ_1 . So we still solve problem corresponding to (27).

⁹When user (1,1) is the typical user, it can be verified that ω_s and μ_s defined in (41) are $(\omega_r-\varphi_{1,1})$ and $(\mu_r-\theta_{1,1})$, respectively, and $\frac{1}{1}1_{11}^T\beta_1\alpha_r$ in (39) is $\alpha_r\beta_{1,1}$.

by a 1-sparse recovery problem, and thus we have $\Upsilon_1 \geq \mathcal{O}(\log(M))$. As shown before, J_1 virtual single-antenna users share the same blocks and can be processed simultaneously. In addition, the first block is also used for Phase II. Hence the total pilot overhead required for user 1 should satisfy $\tau_1 = \sum_{i=1}^{\Upsilon_1} V_1^{(i)} = V_1^{(1)} + \sum_{i=2}^{\Upsilon_1} V_1^{(i)} \geq \mathcal{O}(J_1 \log(Q_1)) + (\mathcal{O}(\log(M)) - 1)J_1$.

For the other users $2 \le k \le K$, we have the inequalities $V_k^{(1)} \ge \mathcal{O}(J_k \log(Q_k))$ and $V_k^{(i)} \ge J_k$, for the same reasons as for user 1. As before, the angle estimation problem connected with (67) can be treated as a 1-sparse recovery problem, and J_k virtual single-antenna users simultaneously share the same blocks, where the number of time blocks for user ksatisfies $\Upsilon_k \geq \mathcal{O}(\log(M)/L)$. Therefore, the total number of pilot symbols required for user k should satisfy $au_k =$ $V_k^{(1)} + \sum_{i=2}^{\Upsilon_k} V_k^{(i)} \ge \mathcal{O}(J_k \log(Q_k)) + (\mathcal{O}(\log(M)/L) - 1)J_k.$ Finally, the overall pilot overhead for the multi-antenna users is given by $\mathcal{O}(JK\log(Q) + J\log(M) + (K - Q))$ $1)J\log(M)/L$ – JK. Table I summarizes the total number of pilots of the proposed method and other existing algorithms for full-CSI estimation. It is observed that the proposed method achieves a significant reduction in the pilot overhead for both the single-antenna and multi-antenna user cases, owing to the exploitation of the correlation among different users.

VI. SIMULATION RESULTS

In this section, simulation results are provided to evaluate the performance of the proposed three-stage channel estimation protocol for both the single-antenna user case and multi-antenna user case. We assume that channel gains α_l and $\beta_{k,j}$ follow a complex Gaussian distribution with zero mean and variance of $10^{-3} d_{\rm BR}^{-2.2}$ and $10^{-3} d_{\rm RU}^{-2.8}$, respectively. Here, $d_{\rm BR}$ is defined as the distance between the BS and the RIS, while, $d_{\rm RU}$ is defined as the distance between the RIS and the users. The antenna spacing at the BS and the element spacing at the RIS are assumed to satisfy $d_{\rm BS} = d_{\rm RIS} = \frac{\lambda_c}{2}$. The random Bernoulli matrix is chosen as the initial RIS phase shift training matrix E, i.e., the elements are selected from $\{-1,+1\}$ with equal probability [16]. The transmitted power is set to p = 1 W. It is assumed that the propagation angles change every ten channel coherence blocks, while the gains change for each coherence block. Unless otherwise specified, for the single-antenna user case, the dimensions of the UPAs deployed on the BS and the RIS are $N_1 = N_2 = 10$ and $M_1 = M_2 = 10$, respectively. $d_{\rm BR}$ and $d_{\rm RU}$ are set to 10 m and 100 m [16], respectively. The number of users is set to K=4. The number of scatterers between the BS and the RIS, and that between the RIS and users are set to L=5 and $J_1=\cdots=J_K=4$. For the multi-antenna user case, the corresponding parameter settings are $N_1 = N_2 = 8$, $M_1 = M_2 = 8$, $d_{\rm BR} = 80$ m, $d_{\rm RU} = 40$ m, L = 3 and $J_1 = \cdots J_k = 2$. In addition, we set the number of users to K=6 and all the users adopt 36-antenna UPAs with 6 rows and 6 columns, i.e., $Q_{k1} = Q_{k2} = 6$ for $\forall k \in \mathcal{K}$. The antenna spacing at the user equipments still satisfies $d_{\rm UE} = \frac{\lambda_c}{2}$. The normalized mean square error (NMSE) is chosen as the main metric for evaluating estimation performance, which is defined by $\text{NMSE} = \mathbb{E}\{(\sum_{k=1}^K ||\widehat{\mathbf{G}}_k - \mathbf{G}_k||_F^2)/(\sum_{k=1}^K ||\mathbf{G}_k||_F^2)\}.$ We compare the proposed three-stage channel estimation protocol with the following channel estimation methods, in which Direct-OMP [13] and DS-OMP [16] were developed for the single-antenna user case while CS-EST OMP [18] was developed for the multi-antenna user case.

- Direct-OMP [13]: By directly formulating the VAD representation of the cascaded channel as a sparse recovery problem using the vectorization operation, the authors in [13] used OMP to reconstruct the channels. We extend this method to UPA-Type BS in our simulation.
- DS-OMP [16]: By exploiting the common row-block sparsity and common column-block sparsity of the cascaded channel to formulate a sparse recovery problem, the authors in [16] adopted OMP to reconstruct the channels.
- CS-EST OMP [18]: The authors of [18] proposed an OMP-based three-stage channel estimation in ULA-type MIMO case, which estimated AoDs at the users in Stage I, AoAs at the BS in Stage II, and cascaded channel gains in Stage III. We extend the method in [18] to UPA -type MIMO case and regard it as the benchmark.
- Proposed full-CSI: During the first coherence block, full CSI for all users is estimated using Algorithm 2 in Stage I and Algorithm 3 in Stage II assuming a UPA-type RIS and a UPA-type BS. OMP is adopted to solve the sparse recovery problems in these two stages.
- Oracle full-CSI: This method is treated as the performance upper bound of the Proposed full-CSI method assuming that perfect angle information is known by the BS, providing perfect knowledge of the support of the sparsity recovery problems. In this case, the channels are estimated using the LS estimator in Stage I and Stage II.
- Proposed gains-only: During the remaining coherence blocks, only the gains are updated using the LS method shown in Section IV for Stage III. Here, the angle information is known and estimated using the proposed full-CSI method with an average pilot overhead of T=15 (The number of pilots for typical user, i.e., τ_1 , is set to 36 in Stage I, while that for other users, i.e., τ_k , for $2 \le k \le K$, are set to 8 in Stage II).
- Oracle gains-only: This method is regarded as the performance upper bound of the Proposed gains-only method during the remaining coherence blocks, and assumes that the BS perfectly knows the angle information when using the LS estimator.

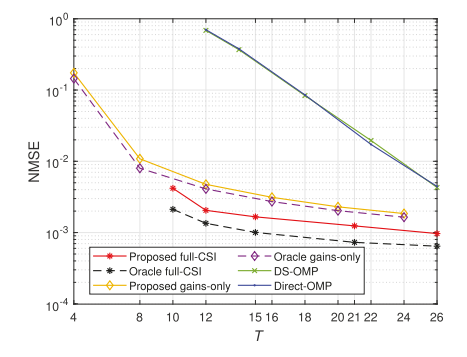
A. Single-Antenna User Case

In this subsection, the following four figures compare the performance of different estimation methods for the single-antenna user case. In particular, due to the different number of pilots allocated to the typical user and other users in the first coherence block for the Proposed full-CSI method, we consider the users' average pilot overhead as a measure of pilots, denoted as T. To reduce the error propagation, 10 we allocate more pilots to the typical user and fewer pilots to the

 $^{^{10}}$ As shown in Section III, the estimation error of the typical user in Stage I leads to unavoidable error propagation for the estimation of other users in Stage II.

Case	Methods	Pilot Overhead
Single-antenna User	Proposed Full-CSI Estimation	$O(J\log(M) + (K-1)J\log(M)/L)$
Single-antenna User	Direct-OMP [13]	$\mathcal{O}(JLK\log(MN)/N)$
Single-antenna User	DS-OMP [16]	$O(JK\log(M))$
Single-antenna User	Row-Structure OMP [15]	$O(JK\log(M))$
Multi-antenna User	Extension of the proposed method	$O(JK\log(Q) + J\log(M) + (K-1)J\log(M)/L) - JK$
Multi-antenna User	CS-EST OMP [18]	$O(JK\log(Q) + JLK\log(MJL)/N)$

TABLE I Total Number of Pilots of Various Methods



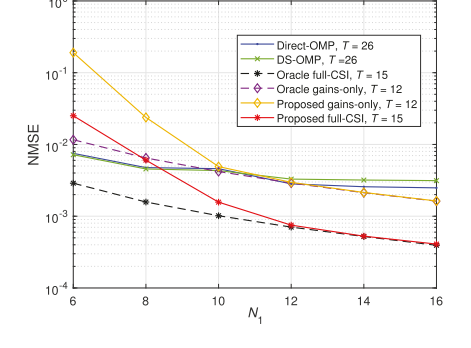


Fig. 2. NMSEs vs. Average pilot overhead T of each user with SNR = 0 dB.

Fig. 3. NMSEs vs. Number of antennas at BS side: $N=N_1\times N_2,$ $N_1=N_2.$

other users. Specifically, in Fig. 3, Fig. 4, and Fig. 5, 36 pilots and 8 pilots are allocated to the typical user and the other users, respectively, thus the average number of pilots for the proposed method is given by T=15.

Fig. 2 illustrates the relationship between NMSE performance and pilot overhead of the various methods, where the signal-to-noise ratio (SNR) is set to 0 dB. We increase the pilot overhead for the typical user mainly for less error propagation. It can be clearly seen that an increase in the number of pilots improves the performance of all algorithms. In order to achieve the same estimation performance, e.g., $NMSE = 10^{-2}$, the required average pilot overhead of the Proposed full-CSI method is much lower than the methods in [13] and [16] during the first coherence block. On the other hand, during the remaining coherence blocks, we note that the Proposed gains-only method only needs T=12 pilots to achieve the same performance as the Direct-OMP and DS-OMP methods with T=26. Additionally, it is observed that the Proposed gains-only method performs generally the same as its upper bound, i.e., Oracle gains-only method, which implies that the Proposed full-CSI method with the average pilot overhead T = 15 during the first coherence block can provide accurate angle estimation information for the Proposed gains-only method to estimate the updated channel gains during the remaining coherence blocks.

Fig. 3 depicts the NMSE performance as a function of the number of antennas at the BS, where we set the SNR to 0 dB and assume $N_1 = N_2$. It can be observed that as the number of antennas at the BS increases, the estimation accuracy of the Proposed full-CSI method with fewer average

pilots, T = 15 (36 pilots allocated to the typical user and 8 pilots allocated to the other users), is improved significantly, and achieves nearly the same performance as the Oracle full-CSI method when N is larger than 144 (12 \times 12). This is because the Proposed full-CSI method must first estimate the number of scatterers in the RIS-BS link from the received signal. The estimation accuracy of this step is determined by the asymptotic property shown in Lemma 2 and the resolution of the rotation matrices defined in (20). The asymptotic property in Lemma 2 requires that both N_1 and N_2 be sufficiently large. In addition, we observe the gap between the Proposed gains-only method and the Oracle gains-only method is large when N=36 (6×6). This behavior illustrates that with small scale antenna array, the Proposed full-CSI method provides inaccurate angle estimation information for the estimation of gains during the remaining coherence blocks, which deteriorates the estimation accuracy of the Proposed gains-only method further. Fortunately, with the increase of the number of antennas, the gap becomes marginal, which means that the angle information has been estimated perfectly in the first coherence block with large scale antenna array.

Fig. 4 illustrates the NMSE performance of algorithms with different pilot overhead versus the number of scatterers in the RIS-BS link, where the SNR is set to 0 dB. As shown in Fig. 4, the estimation accuracy decreases as the number of scatterers increases. The reasons for this behavior can be summarized as follows. First, the number of unknown parameters (angles and gains) to be estimated increases, and thus the OMP-based estimation performs worse for the same pilot overhead. Second, since the number of scatterers is unknown in our

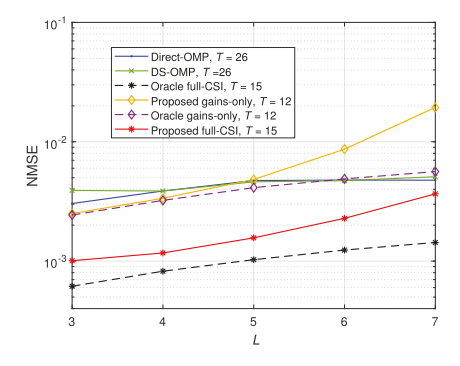


Fig. 4. NMSEs vs. Number of scatterers in RIS-BS link.

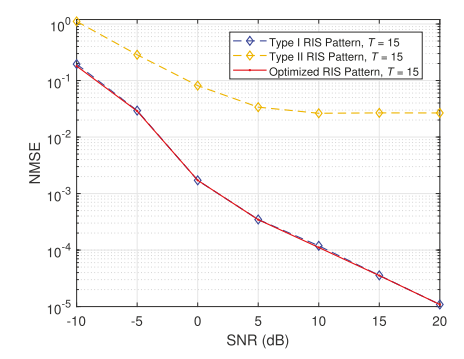


Fig. 5. Performance of Optimized vs. Non-Optimized RIS phase shift training matrices

Proposed full-CSI UPA-type based method, the estimation accuracy of the Proposed full-CSI method is relatively more sensitive to an increase of the number of scatterers than the other methods, which further deteriorates the performance of the Proposed gains-only method in the remaining coherence blocks. By contrast, the NMSEs of the DS-OMP method and the Direct-OMP method with T=26 pilots increases only moderately with the increase of the number of scatterers since the parameters including the numbers of scatterers between the RIS-BS link and the user-RIS link are known by BS for these two methods.

Fig. 5 illustrates whether the optimization of the RIS phase shift training matrix E provides a significant benefit for the estimation performance. "Type I RIS Pattern" refers to choosing the random Bernoulli matrix as the training matrix, i.e., generating the initial training matrix with elements from $\{-1, +1\}$ with equal probability [16]. "Type II RIS Pattern" refers to generating the initial training matrix with elements as $[\mathbf{e}_t]_m = \exp(\mathrm{i}\angle(a+\mathrm{i}b))$ where a and b follow independent and identically uniform distribution $\mathcal{U}(0,1)$. It is observed that the performance of the Type I training matrix is essentially the same as that of the optimized training matrix, and far outperforms that of the Type II training matrix. This behavior can be explained by exploring the mutual coherence property of the equivalent sensing matrices for problems associated with (28) and (48). For a given matrix D, the maximal coherence of **D**, denoted as $\mu(\mathbf{D})$, is defined as

$$\mu(\mathbf{D}) = \max_{i \neq j} \frac{|\mathbf{D}_{(:,i)}^{\mathrm{H}} \mathbf{D}_{(:,j)}|}{||\mathbf{D}_{(:,j)}||||\mathbf{D}_{(:,j)}||},$$
(68)

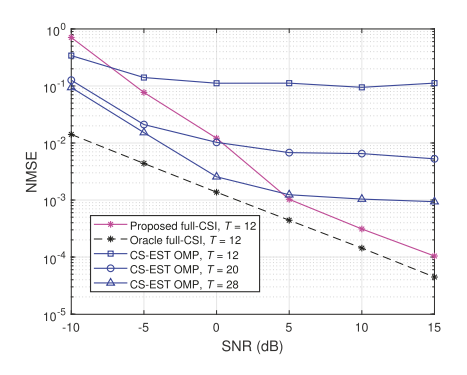


Fig. 6. NMSEs vs. SNR.

which is the largest absolute inner product between any two columns of \mathbf{D} . According to the compressive sensing theory [32], the sensing matrix with smaller $\mu(\mathbf{D})$ could provide better recovery performance for sparse vectors. The random Bernoulli matrix, which is a typical sensing matrix with lower correlation of its columns and satisfies the constant modulus constraint, is chosen as the Type I training matrix. Furthermore, numerical results validate that the maximal coherence of the sensing matrices generated by the Type I training matrix is significantly lower than that generated by the Type II training matrices, and nearly the same as that generated by the optimized training matrix. Since optimization of the training matrix requires extra computational complexity, this result suggests that "Type I RIS Pattern" be chosen for the RIS phase shift training matrix.

B. Multi-Antenna User Case

In this subsection, the NMSE and weighted sum rate (WSR) of the multi-antenna user case are respectively shown in Fig. 6 and Fig. 7 by using different estimation methods. The users' average pilot overhead is considered for the proposed method in the multi-antenna user case, similar to that in the single-antenna user case. Specifically, for estimating the AoDs at the users, we allocate 10 slots to all the users including the typical user and other users in Phase I, i.e., $V_k^{(1)}=10$ for $\forall k\in\mathcal{K}$. In phase II, additional 3 blocks of time slots are allocated to the typical user and each block has 4 slots, i.e., $V_1^{(2)}=V_1^{(3)}=V_1^{(4)}=4$. Therefore, the pilot overhead allocated to the typical user and other users are 22 and 10, respectively. The average pilot overhead for the proposed method is given by T=12. In addition, for fairness, CS-EST OMP consumes the same number of slots for the estimation of AoDs at the

Fig. 6 displays the NMSE performance of different methods versus SNR. It is observed that the gap between the Proposed full-CSI method and its upper bound, i.e., the Oracle full-CSI method, becomes smaller with the increase of SNR. In particular, when the SNR is larger than 5 dB, the NMSE of the proposed method with T=12 exceeds that of the CE-EST OMP method with T=28, and has the same trend as that of the Oracle full-CSI method, i.e., the NMSEs decrease linearly with the SNR. This behavior implies the angle information can be obtained accurately by the Proposed full-CSI method at

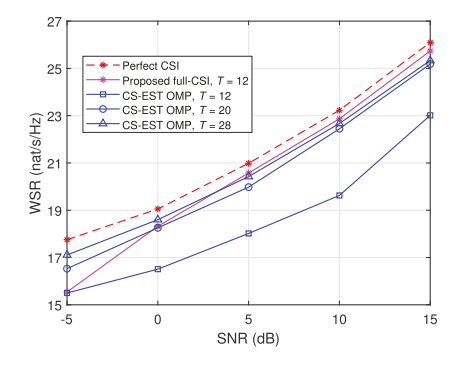


Fig. 7. WSR vs. SNR.

large SNR region. In this case, the NMSE differences between the proposed method and its upper bound mainly results from the estimation errors of channel gain information. By contrast, the NMSE of the CS-EST OMP method still has a performance bottleneck in the high SNR region even under the scenario of up to 28 pilots per user.

Fig. 7 shows the WSR performance of the MU MIMO system based on the channels estimated using different algorithms. The weighting factors, the maximum BS power, and the number of data streams are set to $\varpi_k = 1$ for $\forall k \in \mathcal{K}$, $P_{max} = 1$ W, and d = 16, respectively. The details of the calculation for WSR can refer to [33, Appendix D]. In Fig. 7, the case with perfect CSI is adopted as the upper bound of the Proposed full-CSI and CE-EST OMP methods. As can be observed, the WSR achieved by the proposed method with T = 12 pilots is always larger than that achieved by the CS-EST OMP method with the same number of pilots of T=12. When SNR = 5 dB, the proposed method outperforms the other three CS-EST OMP methods. To achieve the same WSR, the pilot overhead required by the proposed method is less than half that of the CE-EST OMP method. With the further increase of the SNR, the gap between the proposed method and the upper bound becomes smaller gradually, which implies that extension of the proposed full-CSI method to the multi-antenna user case can achieve high estimation accuracy.

VII. CONCLUSION

In this paper, we adopted a novel three-stage uplink channel estimation protocol that leads to a significant reduction in the number of pilots for a UPA-type RIS-aided mmWave system with a UPA-type BS. The proposed estimation methods were developed starting from the single-antenna user case, and were shown to fully exploit the correlation among the channels of different users. To reduce the power leakage problem during the common AoA estimation in Stage I, a low-complexity 1-D search method was developed. Then we extended the protocol to the UPA-type multi-antenna user case. An OMP-based method was proposed for estimation of the AoDs at the users. Numerical results showed that choosing the random Bernoulli matrix as the RIS training matrix has near-optimal performance. Simulation results validated that the proposed methods outperform other existing algorithms in

terms of pilot overhead. In addition, the proposed algorithms approach the genie-aided upper bound in the high SNR regime.

Future studies can include the application of learning-based approaches to our proposed channel estimation protocol. With the increase of the number of RIS elements and BS/users antennas, the computational complexity for the conventional model-driven estimation methods becomes inevitably high. This fact motivates the development of data-driven or hybrid approaches for the proposed protocol in the future, which can obtain the estimates with reduced complexity, and the correlation relationship among multi-user cascaded matrices is still utilized for pilot overhead reduction.

APPENDIX

Appendix can be found in [33, Appendix].

REFERENCES

- Z. Peng, G. Zhou, C. Pan, and H. Ren, "Channel estimation for RISaided mmWave MIMO system from 1-sparse recovery perspective," in Proc. IEEE Global Commun. Conf. (GLOBECOM), Dec. 2022.
- [2] Q. Wu and R. Zhang, "Towards smart and reconfigurable environment: Intelligent reflecting surface aided wireless network," *IEEE Commun. Mag.*, vol. 58, no. 1, pp. 106–112, Jan. 2020.
- [3] M. Di Renzo et al., "Smart radio environments empowered by reconfigurable intelligent surfaces: How it works, state of research, and the road ahead," *IEEE J. Sel. Areas Commun.*, vol. 38, no. 11, pp. 2450–2525, Nov. 2020.
- [4] C. Pan et al., "Reconfigurable intelligent surfaces for 6G systems: Principles, applications, and research directions," *IEEE Commun. Mag.*, vol. 59, no. 6, pp. 14–20, Jun. 2021.
 [5] X. You et al., "Towards 6G wireless communication networks: Vision,
- [5] X. You et al., "Towards 6G wireless communication networks: Vision, enabling technologies, and new paradigm shifts," Sci. China Inf. Sci., vol. 64, no. 1, Jan. 2021, Art. no. 110301.
- [6] C. Pan et al., "Intelligent reflecting surface aided MIMO broadcasting for simultaneous wireless information and power transfer," *IEEE J. Sel. Areas Commun.*, vol. 38, no. 8, pp. 1719–1734, Aug. 2020.
- [7] C. Pan et al., "Multicell MIMO communications relying on intelligent reflecting surfaces," *IEEE Trans. Wireless Commun.*, vol. 19, no. 8, pp. 5218–5233, Aug. 2020.
- [8] A. L. Swindlehurst, G. Zhou, R. Liu, C. Pan, and M. Li, "Channel estimation with reconfigurable intelligent surfaces—A general framework," *Proc. IEEE*, vol. 110, no. 9, pp. 1312–1338, Sep. 2022.
- [9] B. Zheng, C. You, W. Mei, and R. Zhang, "A survey on channel estimation and practical passive beamforming design for intelligent reflecting surface aided wireless communications," 2021, arXiv:2110.01292.
- [10] Y.-C. Liang, J. Chen, R. Long, Z.-Q. He, X. Lin, and C. Huang, "Reconfigurable intelligent surfaces for smart wireless environments: Channel estimation, system design and applications in 6G networks," Sci. China Inf. Sci., vol. 64, no. 10, Oct. 2021, Art. no. 200301.
- [11] Q.-U.-U. Nadeem, A. Kammoun, A. Chaaban, M. Debbah, and M.-S. Alouini, "Intelligent reflecting surface assisted wireless communication: Modeling and channel estimation," 2019, arXiv:1906.02360.
- [12] Z. Wang, L. Liu, and S. Cui, "Channel estimation for intelligent reflecting surface assisted multiuser communications: Framework, algorithms, and analysis," *IEEE Trans. Wireless Commun.*, vol. 19, no. 10, pp. 6607–6620, Jun. 2020.
- [13] P. Wang, J. Fang, H. Duan, and H. Li, "Compressed channel estimation for intelligent reflecting surface-assisted millimeter wave systems," *IEEE Signal Process. Lett.*, vol. 27, pp. 905–909, 2020.
- [14] J. He, H. Wymeersch, and M. Juntti, "Channel estimation for RIS-aided mmWave MIMO systems via atomic norm minimization," *IEEE Trans. Wireless Commun.*, vol. 20, no. 9, pp. 5786–5797, Sep. 2021.
- [15] J. Chen, Y.-C. Liang, H. Victor Cheng, and W. Yu, "Channel estimation for reconfigurable intelligent surface aided multi-user MIMO systems," 2019, arXiv:1912.03619.
- [16] X. Wei, D. Shen, and L. Dai, "Channel estimation for RIS assisted wireless communications—Part II: An improved solution based on doublestructured sparsity," *IEEE Commun. Lett.*, vol. 25, no. 5, pp. 1403–1407, May 2021.

- [17] G. Zhou, C. Pan, H. Ren, P. Popovski, and A. L. Swindlehurst, "Channel estimation for RIS-aided multiuser millimeter-wave systems," *IEEE Trans. Signal Process.*, vol. 70, pp. 1478–1492, 2022.
- [18] T. Lin, X. Yu, Y. Zhu, and R. Schober, "Channel estimation for IRS-assisted millimeter-wave MIMO systems: Sparsity-inspired approaches," *IEEE Trans. Commun.*, vol. 70, no. 6, pp. 4078–4092, Jun. 2022.
- [19] X. Wu, X. Yang, S. Ma, B. Zhou, and G. Yang, "Hybrid channel estimation for UPA-assisted millimeter-wave massive MIMO IoT systems," *IEEE Internet Things J.*, vol. 9, no. 4, pp. 2829–2842, Feb. 2022.
- [20] C. Hu, L. Dai, T. Mir, Z. Gao, and J. Fang, "Super-resolution channel estimation for mmWave massive MIMO with hybrid precoding," *IEEE Trans. Veh. Technol.*, vol. 67, no. 9, pp. 8954–8958, Sep. 2018.
- [21] D. Fan et al., "Angle domain channel estimation in hybrid millimeter wave massive MIMO systems," *IEEE Trans. Wireless Commun.*, vol. 17, no. 12, pp. 8165–8179, Dec. 2018.
- [22] X. Wu, S. Ma, X. Yang, and G. Yang, "Clustered sparse Bayesian learning based channel estimation for millimeter-wave massive MIMO systems," *IEEE Trans. Veh. Technol.*, early access, Aug. 4, 2022.
- [23] R. Méndez-Rial, C. Rusu, N. González-Prelcic, A. Alkhateeb, and R. W. Heath, Jr., "Hybrid MIMO architectures for millimeter wave communications: Phase shifters or switches?" *IEEE Access*, vol. 4, pp. 247–267, 2016.
- [24] X. Hu, C. Zhong, Y. Zhang, X. Chen, and Z. Zhang, "Location information aided multiple intelligent reflecting surface systems," *IEEE Trans. Commun.*, vol. 68, no. 12, pp. 7948–7962, Dec. 2020.
- [25] V. Raghavan et al., "Statistical blockage modeling and robustness of beamforming in millimeter-wave systems," *IEEE Trans. Microw. Theory Techn.*, vol. 67, no. 7, pp. 3010–3024, Jul. 2019.
- [26] H. Xie, F. Gao, S. Zhang, and S. Jin, "A unified transmission strategy for TDD/FDD massive MIMO systems with spatial basis expansion model," *IEEE Trans. Veh. Technol.*, vol. 66, no. 4, pp. 3170–3184, Apr. 2017.
- [27] M. Wax and A. Adler, "Detection of the number of signals by signal subspace matching," *IEEE Trans. Signal Process.*, vol. 69, pp. 973–985, 2021.
- [28] V. I. Slyusar, "A family of face products of matrices and its properties," Cybern. Syst. Anal., vol. 35, no. 3, pp. 379–384, May 1999.
- [29] X.-D. Zhang, Matrix Analysis and Applications. Cambridge, U.K.: Cambridge Univ. Press, 2017.
- [30] E. J. Candès, J. Romberg, and T. Tao, "Robust uncertainty principles: Exact signal reconstruction from highly incomplete frequency information," *IEEE Trans. Inf. Theory*, vol. 52, no. 2, pp. 489–509, Eab. 2006.
- [31] O. El Ayach, S. Rajagopal, S. Abu-Surra, Z. Pi, and R. W. Heath, Jr., "Spatially sparse precoding in millimeter wave MIMO systems," *IEEE Trans. Wireless Commun.*, vol. 13, no. 3, pp. 1499–1513, Mar. 2014.
- [32] M. F. Duarte and Y. C. Eldar, "Structured compressed sensing: From theory to applications," *IEEE Trans. Signal Process.*, vol. 59, no. 9, pp. 4053–4085, Sep. 2011.
- [33] Z. Peng et al., "Channel estimation for RIS-aided multi-user mmWave systems with uniform planar arrays," 2022, *arXiv:2208.07069*.



Gui Zhou (Member, IEEE) received the B.S. and M.E. degrees from the School of Information and Electronics, Beijing Institute of Technology, Beijing, China, in 2015 and 2019, respectively, and the Ph.D. degree from the School of Electronic Engineering and Computer Science, Queen Mary University of London, U.K., in 2022. She is currently a Humboldt Post-Doctoral Research Fellow with the Institute for Digital Communications, Friedrich-Alexander-University Erlangen-Nürnberg (FAU), Erlangen, Germany. Her major

research interests include reconfigurable intelligent surfaces (RIS) and array signal processing.



Cunhua Pan (Member, IEEE) received the B.S. and Ph.D. degrees from the School of Information Science and Engineering, Southeast University, Nanjing, China, in 2010 and 2015, respectively.

From 2015 to 2016, he was a Research Associate at the University of Kent, U.K. He held a post-doctoral position at the Queen Mary University of London, U.K., from 2016 to 2019, where he was a Lecturer from 2019 to 2021. Since 2021, he has been a Full Professor with Southeast University. He has published over 120 IEEE journal articles. His

research interests include reconfigurable intelligent surfaces (RIS), intelligent reflection surface (IRS), ultra-reliable low latency communication (URLLC), machine learning, UAV, the Internet of Things, and mobile edge computing. He serves as a TPC Member for numerous conferences, such as ICC and GLOBECOM, and the Student Travel Grant Chair for ICC 2019. He received the IEEE ComSoc Leonard G. Abraham Prize in 2022 and IEEE ComSoc Asia-Pacific Outstanding Young Researcher Award in 2022. He is the Workshop Chair of IEEE WCNC 2024 and a TPC Co-Chair of IEEE ICCT 2022. He is currently an Editor of IEEE TRANSACTIONS ON VEHICULAR TECHNOLOGY, IEEE WIRELESS COMMUNICATION LETTERS, IEEE COM-MUNICATIONS LETTERS, and IEEE ACCESS. He serves as a Guest Editor for IEEE JOURNAL ON SELECTED AREAS IN COMMUNICATIONS on the Special Issue on xURLLC in 6G: Next Generation Ultra-Reliable and Low-Latency Communications. He also serves as a Leading Guest Editor for IEEE JOURNAL OF SELECTED TOPICS IN SIGNAL PROCESSING Special Issue on Advanced Signal Processing for Reconfigurable Intelligent Surface-Aided 6G Networks, a Leading Guest Editor for IEEE Vehicular Technology Magazine on the Special Issue on Backscatter and Reconfigurable Intelligent Surface Empowered Wireless Communications in 6G, a Leading Guest Editor for IEEE OPEN JOURNAL OF VEHICULAR TECHNOLOGY on the Special Issue of Reconfigurable Intelligent Surface Empowered Wireless Communications in 6G and Beyond, and a Leading Guest Editor for IEEE Access Special Issue on Reconfigurable Intelligent Surface Aided Communications for 6G and Beyond. He is a Workshop Organizer in IEEE ICCC 2021 on the topic of Reconfigurable Intelligent Surfaces for Next Generation Wireless Communications (RIS for 6G Networks), and a Workshop Organizer in IEEE GLOBECOM 2021 on the topic of Reconfigurable Intelligent Surfaces for future wireless communications. He is also the Workshops and Symposia Officer of Reconfigurable Intelligent Surfaces Emerging Technology Initiative.



Zhendong Peng received the B.S. degree in communication engineering from the University of Electronic Science and Technology of China and the B.Eng. degree (Hons.) in electronics and electrical engineering from the University of Glasgow in 2020. He is currently pursuing the M.S. degree in information and communication engineering with the University of Electronic Science and Technology of China. His major research interests include reconfigurable intelligent surface.



Hong Ren (Member, IEEE) received the B.S. degree in electrical engineering from Southwest Jiaotong University, Chengdu, China, in 2011, and the M.S. and Ph.D. degrees in electrical engineering from Southeast University, Nanjing, China, in 2014 and 2018, respectively. From 2016 to 2018, she was a Visiting Student with the School of Electronics and Computer Science, University of Southampton, U.K. From 2018 to 2020, she was a Post-Doctoral Scholar with the Queen Mary University of London, U.K. She is currently an Associate Professor with

Southeast University. Her research interests include communication and signal processing, including ultra-low latency and high reliable communications, massive MIMO and machine learning. She received the IEEE ComSoc Leonard G. Abraham Prize in 2022.



A. Lee Swindlehurst (Fellow, IEEE) received the B.S. and M.S. degrees in electrical engineering from Brigham Young University (BYU) in 1985 and 1986, respectively, and the Ph.D. degree in electrical engineering from Stanford University in 1991. He was with the Department of Electrical and Computer Engineering, BYU, from 1990 to 2007, where he worked as the Department Chair from 2003 to 2006. During 1996–1997, he held a joint appointment as a Visiting Scholar at Uppsala University and the Royal Institute of Technology in Sweden.

From 2006 to 2007, he was on leave working as the Vice President of Research for ArrayComm LLC, San Jose, CA, USA. Since 2007, he has been a Professor with the Electrical Engineering and Computer Science (EECS) Department, University of California at Irvine, where he worked as the Associate Dean for Research and Graduate Studies with the Samueli School of Engineering from 2013 to 2016, where he is currently the Chair of the EECS Department. During 2014-2017, he was also a Hans Fischer Senior Fellow with the Institute for Advanced Studies, Technical University of Munich. His research interests include array signal processing for radar, wireless communications, and biomedical applications, and he has over 400 publications in these areas. In 2016, he was elected as a Foreign Member of the Royal Swedish Academy of Engineering Sciences (IVA). He received the 2000 IEEE W. R. G. Baker Prize Paper Award, the 2006 IEEE Communications Society Stephen O. Rice Prize in the Field of Communication Theory, the 2006, 2010, and 2021 IEEE Signal Processing Society's Best Paper Awards, the 2017 IEEE Signal Processing Society Donald G. Fink Overview Paper Award, and a Best Paper Award at the 2020 IEEE International Conference on Communications. He was the Inaugural Editor-in-Chief of the IEEE JOURNAL OF SELECTED TOPICS IN SIGNAL PROCESSING.



Petar Popovski (Fellow, IEEE) received the Dipl.-Ing. and M.Sc. degrees in communication engineering from the University of Sts. Cyril and Methodius in Skopje and the Ph.D. degree from Aalborg University in 2005. He is currently a Professor at Aalborg University, where he heads the Section on Connectivity and a Visiting Excellence Chair at the University of Bremen. He authored the book Wireless Connectivity: An Intuitive and Fundamental Guide, published by Wiley in 2020. His research interests include wireless communication and com-

munication theory. He was a Member at Large at the Board of Governors in

IEEE Communication Society 2019–2021. He received an ERC Consolidator Grant in 2015, the Danish Elite Researcher Award in 2016, IEEE Fred W. Ellersick Prize in 2016, IEEE Stephen O. Rice Prize in 2018, Technical Achievement Award from the IEEE Technical Committee on Smart Grid Communications in 2019, the Danish Telecommunication Prize in 2020, and Villum Investigator Grant in 2021. He also serves as a Vice-Chair for the IEEE Communication Theory Technical Committee and the Steering Committee of IEEE Transactions on Green Communications and IEEE Communication Theory Workshop 2019. He is also the Editor-in-Chief of IEEE Journal on Selected Areas in Communications.



Gang Wu (Member, IEEE) received the B.Eng. and M.Eng. degrees from the Chongqing University of Posts and Telecommunications, Chongqing, China, in 1996 and 1999, respectively, and the Ph.D. degree from the University of Electronic Science and Technology of China (UESTC), Chengdu, China, in 2004. Since June 2004, he has been with the UESTC. He is currently a Professor with the National Key Laboratory of Science and Technology on Communications. He was a Research Fellow of the Positioning and Wireless Technology Centre,

Nanyang Technological University, Singapore, from November 2005 to February 2007, and a Visiting Professor with the Georgia Institute of Technology, Atlanta, GA, USA, from October 2009 to September 2010. His research interests include signal processing and resource management for 5G/6G and artificial intelligence for PHY/MAC design in wireless communications systems. He was a co-recipient of the IEEE GLOBECOM 2012 Best Paper Award. He is also an Editor of *Science China Information Sciences*, the Chair of IEEE Comsoc Chengdu Chapter, and the Secretary of the IEEE Chengdu Section.